Cell

Skeletal Muscle PGC-1α1 Modulates Kynurenine Metabolism and Mediates Resilience to Stress-Induced Depression

Leandro Z. Agudelo,[1,8] Teresa Femenía,[1,2,8] Funda Orhan,[3] Margareta Porsmyr-Palmertz,[1] Michel Goiny,[3] Vicente Martinez-Redondo,[1] Jorge C. Correia,[1] Manizheh Izadi,[1] Maria Bhat,[4,5] Ina Schuppe-Koistinen,[4,5] Amanda T. Pettersson,[1] Duarte M.S. Ferreira,[1] Anna Krook,[6] Romain Barres,[6] Juleen R. Zierath,[6,7] Sophie Erhardt,[3] Maria Lindskog,[2,*] and Jorge L. Ruas[1,*]

[1]Department of Physiology and Pharmacology, Molecular and Cellular Exercise Physiology, Karolinska Institutet, 17177 Stockholm, Sweden
[2]Department of Neuroscience, Karolinska Institutet, 17177 Stockholm, Sweden
[3]Department of Physiology and Pharmacology, Neuropsychoimmunology, Karolinska Institutet, 17177 Stockholm, Sweden
[4]AstraZeneca R&D, Innovative Medicines, Personalized Healthcare and Biomarkers, Translational Science Center, Science for Life Laboratory, 17165 Solna, Sweden
[5]Department of Clinical Neuroscience, Karolinska Institutet, 17177 Stockholm, Sweden
[6]Department of Physiology and Pharmacology, Integrative Physiology, Karolinska Institutet, 17177 Stockholm, Sweden
[7]Department of Molecular Medicine and Surgery, Integrative Physiology, Karolinska Institutet, 17177 Stockholm, Sweden
[8]Co-first author
*Correspondence: mia.lindskog@ki.se (M.L.), jorge.ruas@ki.se (J.L.R.)
http://dx.doi.org/10.1016/j.cell.2014.07.051

SUMMARY

Depression is a debilitating condition with a profound impact on quality of life for millions of people worldwide. Physical exercise is used as a treatment strategy for many patients, but the mechanisms that underlie its beneficial effects remain unknown. Here, we describe a mechanism by which skeletal muscle PGC-1α1 induced by exercise training changes kynurenine metabolism and protects from stress-induced depression. Activation of the PGC-1α1-PPARα/δ pathway increases skeletal muscle expression of kynurenine aminotransferases, thus enhancing the conversion of kynurenine into kynurenic acid, a metabolite unable to cross the blood-brain barrier. Reducing plasma kynurenine protects the brain from stress-induced changes associated with depression and renders skeletal muscle-specific PGC-1α1 transgenic mice resistant to depression induced by chronic mild stress or direct kynurenine administration. This study opens therapeutic avenues for the treatment of depression by targeting the PGC-1α1-PPAR axis in skeletal muscle, without the need to cross the blood-brain barrier.

INTRODUCTION

The benefit of physical activity in depression is generally accepted (Lawlor and Hopker, 2001; Melanie et al., 2012), although the mechanisms that mediate these effects remain largely unknown. It is also unclear which components of the exercise program, such as skeletal muscle conditioning, cardiovascular effects, or even psychosocial influences, are therapeutic. PGC-1α transcriptional coactivators are induced in skeletal muscle by exercise (Baar et al., 2002; Ruas et al., 2012; Short et al., 2003) and control many of the adaptations to physical activity. In particular, PGC-1α1 is activated in skeletal muscle by endurance-type activity and promotes mitochondrial biogenesis, fatty acid oxidation, angiogenesis, and resistance to muscle atrophy (Arany, 2008). Transgenic murine models with skeletal muscle-specific PGC-1α1 overexpression (mck-PGC-1α1 mice) show many of the adaptations to endurance-type training, without any exercise interventions (Lin et al., 2002). The mck-PGC-1α1 model has been extensively studied and has a lean, fatigue-resistant phenotype, with no differences at baseline in locomotor activity (Choi et al., 2008).

Depression is a heterogeneous disorder, and the exact neuronal mechanisms causing the disease are yet to be discovered. However, recent work suggests it is accompanied by an imbalance in glutamate transmission and/or decreased synaptic plasticity (Gómez-Galán et al., 2013; Pittenger, 2013; Sanacora et al., 2012).

The modulation of glutamate transmission and plasticity by stress-induced neuroinflammatory pathways may constitute a link between depression and chronic stress (Foy et al., 1987; Liu et al., 2013; Yuen et al., 2012). In particular, the kynurenine pathway of tryptophan degradation is activated by stress as well as directly by inflammatory factors (Gibney et al., 2013; Liu et al., 2013). This pathway accounts for 90% of peripheral tryptophan metabolism and occurs mainly in the liver, kidney, and immune cells (Müller and Schwarz, 2007). Levels of kynurenine (KYN) and its metabolites 3-hydroxykynurenine (3HK) and kynurenic acid (KYNA) in patients are strongly correlated to depression (Claes et al., 2011; Müller and Schwarz, 2007). These compounds have a plethora of effects that could contribute to depression, including modulating neuronal cell death, glutamate

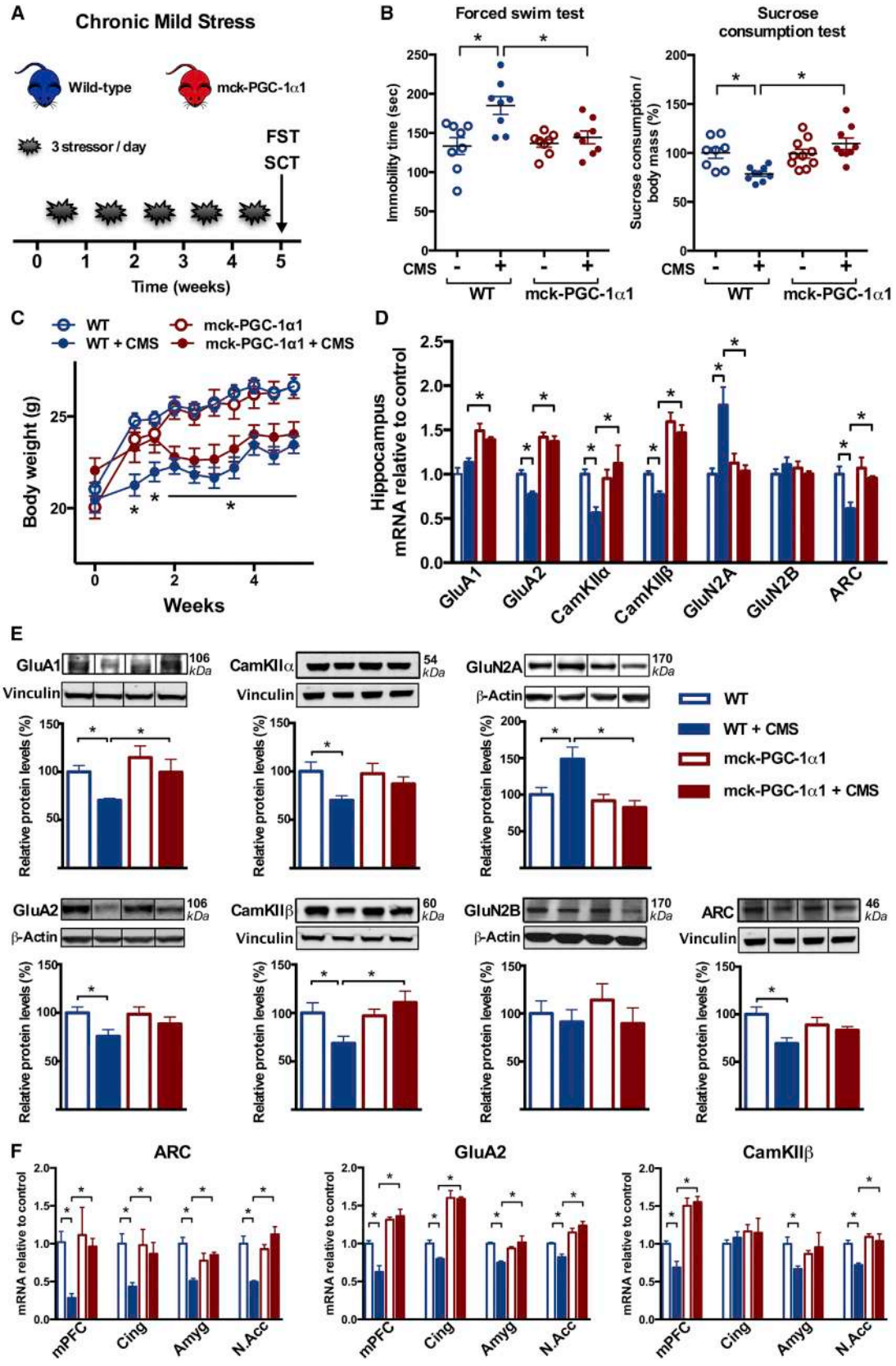

(legend on next page)

transmission, and neuroinflammation (Myint and Kim, 2014; Schwarcz et al., 2012). Approximately 60% of brain KYN comes from the periphery because, as opposed to KYNA, it can readily cross the blood-brain barrier (Fukui et al., 1991; Gál and Sherman, 1980). In the brain, KYN is metabolized to KYNA by astrocytes and to 3HK in microglia and macrophages (Schwarcz et al., 2012).

Here, we show that modulation of skeletal muscle condition through PGC-1α1 expression mediates resilience to stress-induced depressive behavior. Together with PPARα/δ, PGC-1α1 increases the expression of several kynurenine aminotransferases (KATs) in skeletal muscle. Importantly, this shifts peripheral metabolism of stress-induced and exogenous KYN into KYNA, thereby protecting against stress-induced neurobiological mechanisms of depression.

RESULTS

Skeletal Muscle-Specific PGC-1α1 Transgenic Mice Are Resilient to Developing Chronic Mild Stress-Induced Depression

To isolate the effects of skeletal muscle conditioning on depression, we subjected the mck-PGC-1α1 mice to a chronic mild stress (CMS) protocol (Figure 1A). This protocol involves multiple, daily, mild stressors at unpredictable time (Table S1 available online) validated to induce depressive behavior (Willner, 2005). As expected, after 5 weeks of CMS, wild-type (WT) mice displayed depressive behavior as shown by increased immobility time in forced swim tests (FST) (a measure of despair with good predictive value for antidepressant effects) and decreased sucrose consumption (a measure of anhedonia; Figure 1B), when compared to nonstressed control animals. Strikingly, these CMS effects were completely absent in the mck-PGC-1α1 mice (Figure 1B). Genotype had no effect on locomotor activity or baseline sucrose preference (Figures S1A–S1C). Mck-PGC-1α1 mice were not protected from all the effects of CMS and showed decreases in body weight gain similar to WT after the second week (Figure 1C).

To exclude any nonskeletal muscle transgene expression in mck-PGC-1α1 mice, we determined exogenous and endogenous PGC-1α1 levels in several tissues (Figure S1D). We detected PGC-1α1 transgenic expression in skeletal muscle, a small increase in the heart, but not in any of the other analyzed tissues (Figure S1E).

Imbalances in glutamate transmission and decreased synaptic plasticity have been suggested as possible mechanisms of depression (Duman and Aghajanian, 2012; Sanacora et al., 2012). Accordingly, our analysis of synaptic proteins in WT mice after CMS revealed reduced hippocampal expression levels of proteins mediating synaptic plasticity: CamKIIα and CamKIIβ and ARC, as well as the AMPA receptor subunits GluA1 and 2. Expression of the NMDA receptor subunit GluN2B remained unchanged whereas GluN2A protein levels increased after stress (Figures 1D–1F). In agreement with the behavioral test results, none of these stress-induced changes occurred in mck-PGC-1α1 mice (Figures 1D–1F). Similar gene expression profiles were observed in other brain regions (Figures 1F and S1F) known to be involved in depressive disorders (Femenía et al., 2012). Neurotrophic factors also play a role in depression (Anisman and Hayley, 2012; Duman and Monteggia, 2006). After exposure to CMS, only WT mice showed decreased hippocampal transcript levels for BDNF, GDNF, and VEGFA and B, whereas no changes were observed in mck-PGC-1α1 mice (Figure 2A). Nerve-growth factor (NGF) levels did not change in any experimental group (Figure 2A).

Reduced astrocytic regulation of synaptic function has been proposed to contribute to stress-induced depression (Gómez-Galán et al., 2013; Rajkowska and Miguel-Hidalgo, 2007). Consistent with earlier observations (Banasr et al., 2010), CMS reduced the amount of glial fibrillary acidic protein (GFAP) and excitatory amino acid transporter 1 (EAAT1) protein, but not EAAT2 protein abundance in WT mice (Figures 2B and 2C). Baseline GFAP transcript levels were higher in hippocampi of mck-PGC-1α1 mice than in controls, but remained unaffected by CMS (Figure 2B). Further supporting its effect on glutamatergic transmission, CMS decreased the mRNA levels of glutamine synthetase (GLNS) in the hippocampus of WT mice, whereas we observed the opposite effect in mck-PGC-1α1 mice after CMS (Figure 2D). When assessing gene expression of astrocytic proteins in other brain regions, a more complex picture emerged (Figure S2A), suggesting that astrocyte response is a fine-tuned result of many signaling pathways.

We next analyzed the expression of structural synaptic genes known to be decreased in patients with depression (Kang et al., 2012; Tochigi et al., 2008). After CMS, we observed a reduction in the hippocampus and mPFC expression levels of calmodulin-2, synapsin-3, and Rab3A, of WT mice (Rab4B and β-tubulin were also decreased in mPFC), whereas these levels were unchanged in mck-PGC-1α1 mice (Figures S2B and S2C). Collectively, these results indicate that PGC-1α1 expression in skeletal muscle protects synaptic transmission and plasticity from stress-induced alterations, rendering mck-PGC-1α1 animals resistant to developing depressive behavior.

Figure 1. Skeletal Muscle-Specific PGC-1α1 Transgenic Mice Are Resilient to Chronic Mild Stress-Induced Depressive Behavior

(A) A chronic mild stress (CMS) protocol was used to induce depressive behavior in wild-type (blue) and muscle-specific PGC-1α1 transgenic mice (mck-PGC-1α1, red).

(B) Immobility time in the forced swim test (left) and sucrose consumption normalized to body weight (right) shown for individual animals (n = 8–10).

(C) Body weight throughout the CMS treatment (n = 8–10).

(D) Analysis of gene expression in hippocampus by quantitative real-time PCR (qRT-PCR) (n = 4–6).

(E) Representative immunoblots and quantification of hippocampal protein levels normalized to loading controls. Proteins were loaded randomly by an experimenter blinded to experimental conditions. Representative images come from the same gel and lines indicate they originate from different lanes (n = 5–8).

(F) Analysis of gene expression in medial prefrontal cortex (mPFC), cingulate cortex (Cing), amygdala (Amyg), and nucleus accumbens (N. Acc) by qRT-PCR (n = 4–6). Scale bars depict mean values expressed as percentage or fold change of wild-type nonstressed and error bars represent SEM, *$p < 0.05$.

See also Figure S1 and Tables S1, S2, and S3.

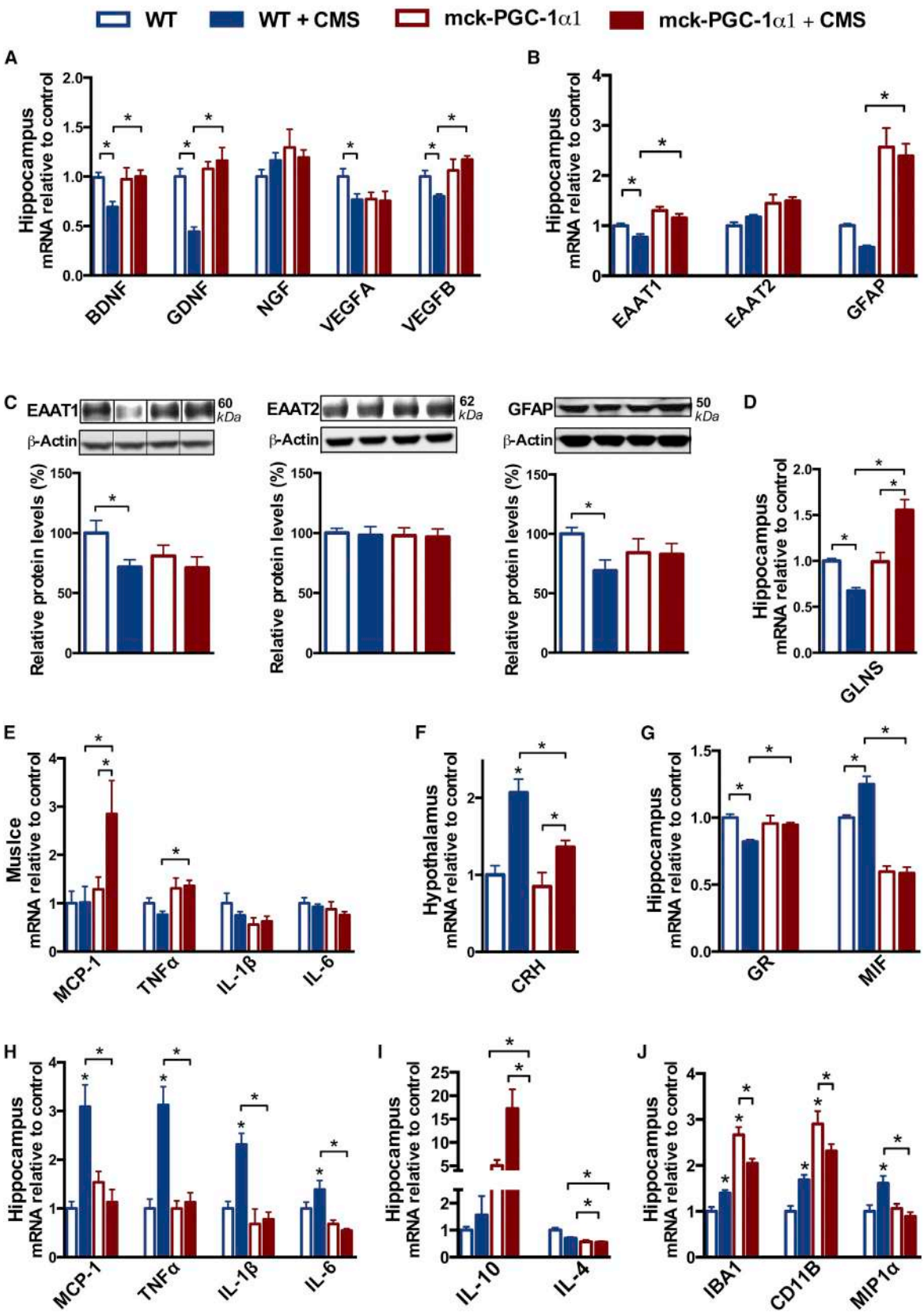

(legend on next page)

Elevated Skeletal Muscle PGC-1α1 Expression Impacts Central Inflammatory Responses to Chronic Mild Stress

Proinflammatory processes and their effects on astrocyte function (McNally et al., 2008) are important promoting factors in the pathogenesis of stress-induced depressive disorders (Anisman and Hayley, 2012; Gibb et al., 2011). Despite the anti-inflammatory properties of PGC-1α1 in muscle (Eisele et al., 2013), chronic exposure of mck-PGC-1α1 mice to unpredictable stress increased skeletal muscle expression of the proinflammatory cytokines MCP-1 and TNFα (Figure 2E). This further indicates that mck-PGC-1α1 mice do respond to stress, despite their resilience to developing depressive behavior. Consistent with this, we observed that CMS increased corticotrophin-releasing hormone (CRH) expression (Deussing and Wurst, 2005; Lloyd and Nemeroff, 2011) in hypothalamus of mck-PGC-1α1 transgenic mice, although to a lesser extent than in WT mice (Figure 2F). WT mice (but not mck-PGC-1α1) responded to CMS with decreased hippocampus glucocorticoid receptor expression (Froger et al., 2004), increased macrophage migration inhibitory factor levels (Figure 2G), and increased levels of stress-induced inflammatory markers (Figures 2H and S2C). Expression of the anti-inflammatory cytokine IL-10 was increased upon CMS in hippocampus of mck-PGC-1α1 mice, whereas IL-4 expression was reduced in all groups compared to WT controls (Figures 2I and S2D). IL-10 and IL-4 levels were unchanged in skeletal muscle (Figure S2E). Lastly, expression of macrophage/microglia activity markers ionized calcium-binding adaptor molecule (IBA1), cyclin-dependent kinase 11b (CD11b), and macrophage inflammatory protein 1α (MIP1α) was increased in hippocampus of WT mice after CMS but reduced (or unchanged) in mck-PGC-1α1 mice under the same conditions (Figure 2J). These results show that although mck-PGC-1α1 mice are sensitive to stress, they are protected from brain neuroinflammation.

PGC-1α1 Induces Expression of Kynurenine Aminotransferases in Skeletal Muscle

To identify pathways that mediate the effects of skeletal muscle PGC-1α1 on the central nervous system we analyzed gene expression array data from in vivo and in vitro muscle PGC-1α1 overexpression (Ruas et al., 2012). This bioinformatic analysis uncovered a putative role for PGC-1α1 in the control of the kynurenine pathway of tryptophan degradation in skeletal muscle (kynurenine pathway; Figures 3A, S3A, and S3B). Conversion of tryptophan to KYN is emerging as a main mediator of stress-induced depression (Dantzer et al., 2008; Müller and Schwarz, 2007). By examining the skeletal muscle expression levels of rate limiting enzymes in the kynurenine pathway, we found that exposure to CMS increased the expression of indoleamine 2, 3-dioxygenase 1 and 2 (IDO1 and IDO2), tryptophan 2, 3-dioxygenase 1 and 2 (TDO1 and TDO2), and kynurenine 3-monooxygenase (KMO) only in WT mice (Figures 3B and 3C). Liver IDO1 expression was increased by CMS in WT mice, to levels higher than those observed in skeletal muscle (Figure S3C). IDO and TDO levels were unchanged in mck-PGC-1α1 skeletal muscle, which instead showed high expression of kynurenine aminotransferases (KAT) 1, 3, and 4, further elevated by CMS (Figures 3D and 3E). These enzymes catalyze the conversion of KYN to KYNA (Han et al., 2010), an end metabolite of this pathway that contrary to KYN cannot cross the blood-brain barrier (BBB) (Fukui et al., 1991). KAT 2 could not be detected in murine skeletal muscle (Figure 3D) and no changes in liver KAT levels were observed (Figure S3C). Although PGC-1α1 levels are slightly elevated in the heart of mck-PGC-1α1 mice, this did not affect cardiac KAT expression (Figure S3D).

Skeletal Muscle PGC-1α1 Enhances Peripheral Metabolism of Kynurenine to Kynurenic Acid during Chronic Mild Stress

Our results suggest that the mck-PGC-1α1 mice are better equipped to metabolize circulating KYN produced in response to CMS. Indeed, exposure to CMS elevated plasma KYN levels in WT, but not in mck-PGC-1α1 mice (Figure 3F). Conversely, only mck-PGC-1α1 mice exposed to CMS showed significantly higher KYNA plasma levels (Figure 3F). Given that KYN crosses the BBB and is rapidly converted to 3HK or KYNA (Fukui et al., 1991; Schwarcz et al., 2012), we measured the levels of these metabolites in the brain. 3HK levels were robustly increased in brains of WT mice after CMS, while unaltered in mck-PGC-1α1 mice (Figure 3G). We observed no differences in brain KYNA levels in any group (Figure 3G). Highlighting the importance of shifting peripheral KYN to KYNA balance, we found a significant correlation between plasma KYN and brain 3HK levels but not with KYNA (Figure 3H). CMS responses increased the expression of enzymes of the kynurenine pathway in brains of WT mice, whereas mck-PGC-1α1 mice were exempt from these changes (Figure S3E). An increased breakdown of kynurenine could lead to tryptophan depletion and result in decreased serotonin levels, a proposed mechanism of depression. However, we did not observe any reduction in tryptophan, serotonin, or its

Figure 2. Skeletal Muscle PGC-1α1 Expression Impacts Central Inflammatory Responses to CMS

(A and B) qRT-PCR gene expression analysis of (A) neurotrophic factors and (B) astrocytic proteins from hippocampus (n = 4–6).

(C) Representative immunoblots and quantification of hippocampal protein levels normalized to loading controls. Proteins were loaded randomly by an experimenter blinded to experimental conditions. Representative images come from the same gel and lines indicate they originate from different lanes (n = 4–8).

(D) Glutamine synthetase (GLNS) mRNA levels in hippocampus (n = 4–6) determined by qRT-PCR.

(E) qRT-PCR analysis of gene expression for inflammatory cytokines in skeletal muscle (n = 4–6).

(F) Corticotrophin-releasing hormone (CRH) gene expression levels in hypothalamus (n = 4–6).

(G) Gene expression levels of glucocorticoid receptor (GR) and microphage migration inhibitory factor (MIF) in hippocampus (n = 4–6).

(H and I) qRT-PCR analysis of gene expression of (H) inflammatory and (I) anti-inflammatory cytokines from hippocampus (n = 4–6).

(J) Analysis of gene expression by qRT-PCR of macrophage/microglial markers from hippocampus (n = 4–6). Scale bars represent mean values and error bars represent SEM. ns, nonsignificant. *p < 0.05.

See also Figure S2 and Tables S2 and S3.

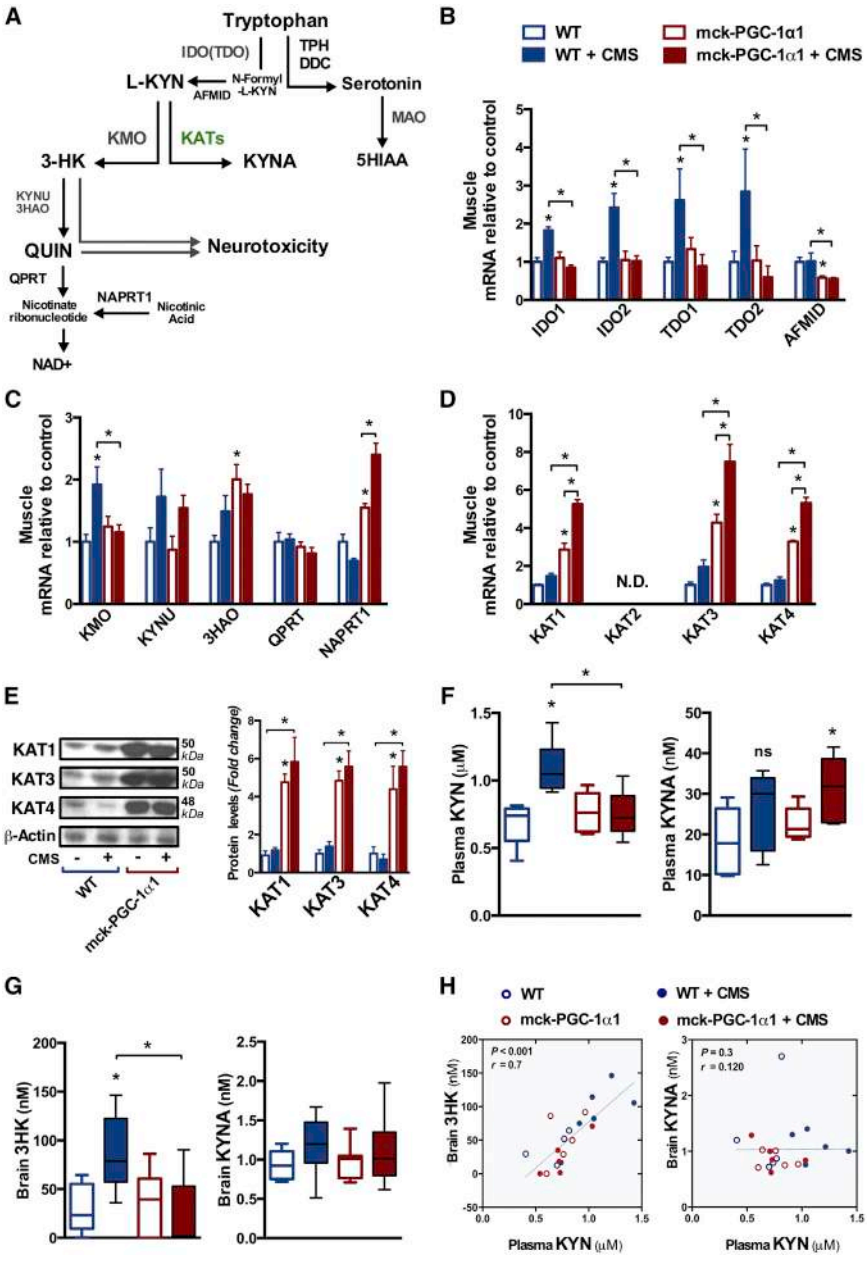

Figure 3. Mck-PGC-1α1 Transgenic Mice Have Enhanced Peripheral Kynurenine Catabolism after Stress

(A) Representation of the kynurenine pathway.

(B–D) Analysis of gene expression by qRT-PCR using primers specific to the indicated genes (n = 4–6).

(E) KAT1, KAT3, and KAT4 protein levels in the gastrocnemius muscle (n = 4). Representative immunoblots (left) and average protein levels relative to controls (right) from gastrocnemius (n = 4).

(F) Box plots of plasma concentrations of kynurenine (KYN) and kynurenic acid (KYNA) (n = 5–7).

(G) Box plots of 3-hydroxykynurenine (3HK) and KYNA concentration in brain tissue (n = 6–10).

(H) Correlation between plasma KYN levels and brain 3HK and KYNA levels with each circle representing an individual animal (n = 20). Scale bars represent mean values and error bars represent SEM. N.D., not detectable. *p < 0.05.

See also Figure S3 and Tables S2 and S3.

metabolite 5-hydroxyindoleacetic acid (5HIAA) levels under any conditions (Figure S3F).

Peripheral Kynurenine Administration Induces Depressive Behavior in Wild-Type, but Not mck-PGC-1α1, Mice

Our data suggest that stress-induced increases in plasma KYN levels have central effects associated with depression. Indeed, KYN plasma levels directly correlated with hippocampal gene expression of proinflammatory markers MCP-1, TNFα, and IL-1β (Figure S4A). We also found that plasma KYN levels inversely correlate with the synaptic changes shown in Figure 1 (Figure 4A). If mck-PGC-1α1 mice are protected from these pathological effects by converting KYN to KYNA in skeletal muscle, this mechanism should also protect from exogenous KYN administration. We determined that a single intraperitoneal 2 mg/kg L-KYN dose results in circulating levels similar to those observed in WT animals exposed to CMS (i.e., 1 μM, see Figure 4F). L-KYN injection resulted in a striking reduction in sucrose consumption in WT mice but not in mck-PGC-1α1 mice (Figure 4B). Moreover, KYN injection in WT mice mimicked the CMS-induced brain pattern of gene expression including proinflammatory (Figure 4C), kynurenine pathway (Figure 4D), and synaptic genes (Figure 4E). This transcriptional signature and the concomitant elevation of plasma KYN levels (Figure 4F) were not observed in mck-PGC-1α1 animals (Figures 4C and 4F). Consistent with our hypothesis, circulating KYNA levels were increased in mck-PGC-1α1 mice after KYN administration (Figure 4F).

Skeletal Muscle-Specific PGC-1α Deletion Sensitizes to KYN-Induced Depressive Behavior

To determine if PGC-1α1 is not only sufficient, but also required for the conversion of KYN to KYNA in skeletal muscle, we next analyzed mice with skeletal muscle-specific genetic deletion of PGC-1α (hereafter MKO-PGC-1α) (Chinsomboon et al., 2009). Loss of PGC-1α expression in skeletal muscle resulted in decreased KAT expression levels (Figures 5A and S5A). When evaluated in sucrose consumption tests, MKO-PGC-1α mice displayed anhedonic behavior even under control conditions

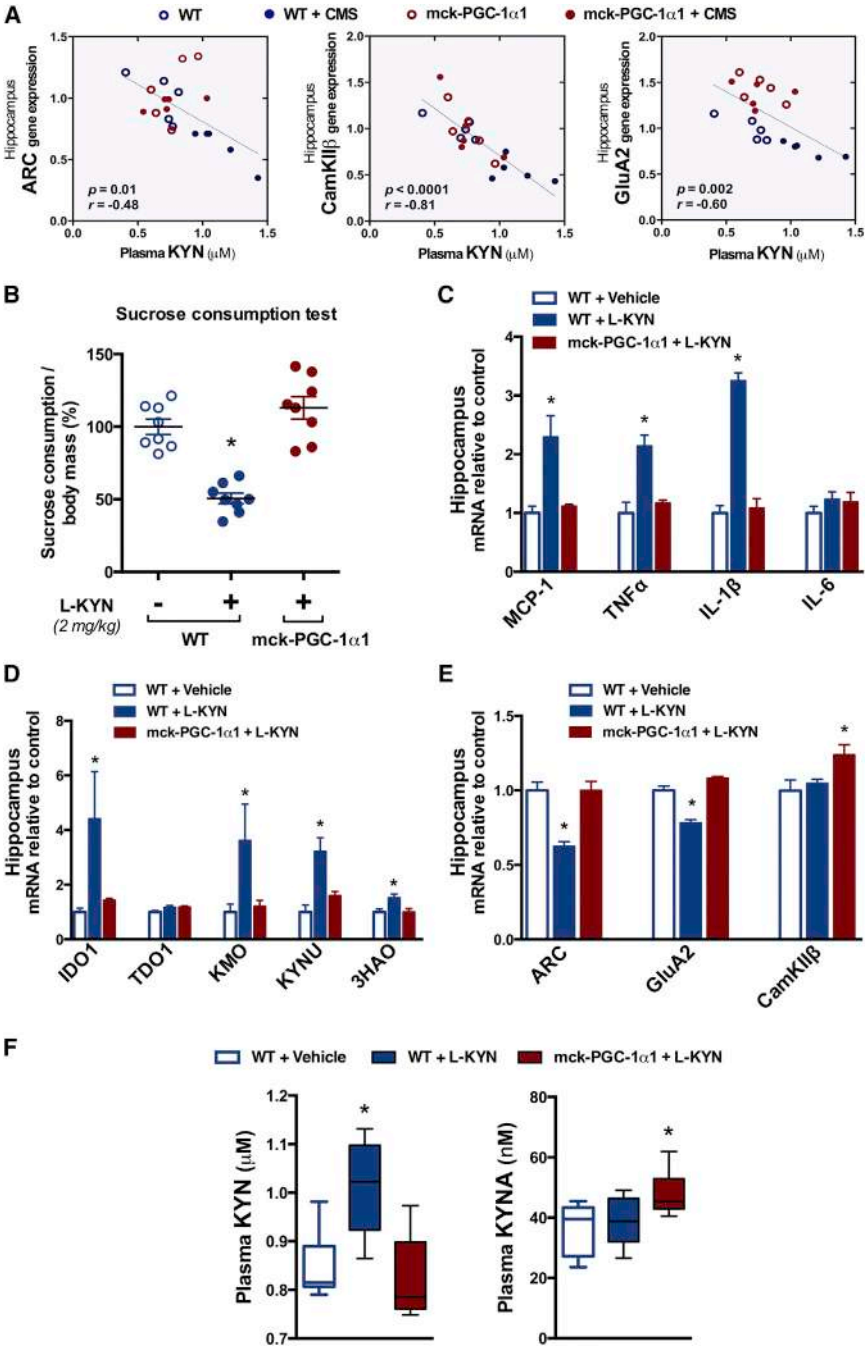

Figure 4. Skeletal Muscle PGC-1α1 Protects from Developing Depressive Behavior Induced by Direct Kynurenine Administration

(A) Correlation between plasma KYN-levels and hippocampal gene expression of indicated genes (same mice as in Figures 1, 2, and 3) with each circle representing an individual mice (n = 20).

(B) Amount of sucrose consumed normalized to body weight after KYN treatment versus vehicle-treated wild-type, unless otherwise indicated (n = 8).

(C–E) mRNA levels of indicated genes in hippocampus from the same animals as in (B).

(F) Plasma concentrations of KYN and KYNA shown as box plots (n = 5–7). Scale bars represent mean values and error bars represent SEM. *p < 0.05.

See also Figure S4 and Table S3.

compared to WT mice (Figures 5B and S5B). This behavior was considerably worsened after exogenous KYN administration and even more pronounced than in the corresponding WT mice (Figure 5C). As before, (Figures 4C–4E), KYN administration induced hippocampal expression of proinflammatory and kynurenine pathway genes in WT mice, but even more clearly in mice lacking muscle PGC-1α (Figures 5D and 5E). The expression of synaptic proteins, with the exception of ARC, was equally reduced in WT and MKO-PGC-1α mice after KYN treatment (Figure 5F). Finally, KYN administration to MKO-PGC-1α mice increased circulating KYN levels even more than in treated WT mice, accompanied by lower KYNA levels (Figure 5G). We did not observe changes in tryptophan or serotonin levels in the MKO-PGC-1α1 mice (Figures S5C and S5D). These findings indicate that acute peripheral KYN administration can drive changes in the brain similar to those induced by CMS, which can be controlled by modulating PGC-1α levels in skeletal muscle.

A PGC-1α1-PPARα/δ Partnership Regulates KAT Expression in Myotubes

To determine if PGC-1α1 effects are cell-autonomous we used primary myotube cultures in gain- and loss-of-function experiments. Myotubes transduced with recombinant adenovirus to overexpress PGC-1α1 (Figure S6A) showed higher KAT1, KAT3, and KAT4 mRNA levels without significant effects on other members of the pathway (Figures 6A and S6B). In agreement with the results obtained in vivo (Figure 5A), MKO-PGC-1α myotubes had decreased KAT1, KAT3, and KAT4 gene expression, which could be rescued by exogenous PGC-1α1 expression (Figure 6B).

PGC-1α coactivators interact with specific DNA-binding transcription factors to exert their biological functions (Lin et al., 2005). Analysis of genomic regions surrounding the KAT1, KAT3, and KAT4 genes revealed an overrepresentation of direct repeat 1 (DR1) sequences (Figure S6C). These elements are recognized by PPARα and δ, well-known PGC-1α1 partners that also increase in skeletal muscle with exercise (Arany, 2008; Schmitt et al., 2003; Wang et al., 2004). In accordance,

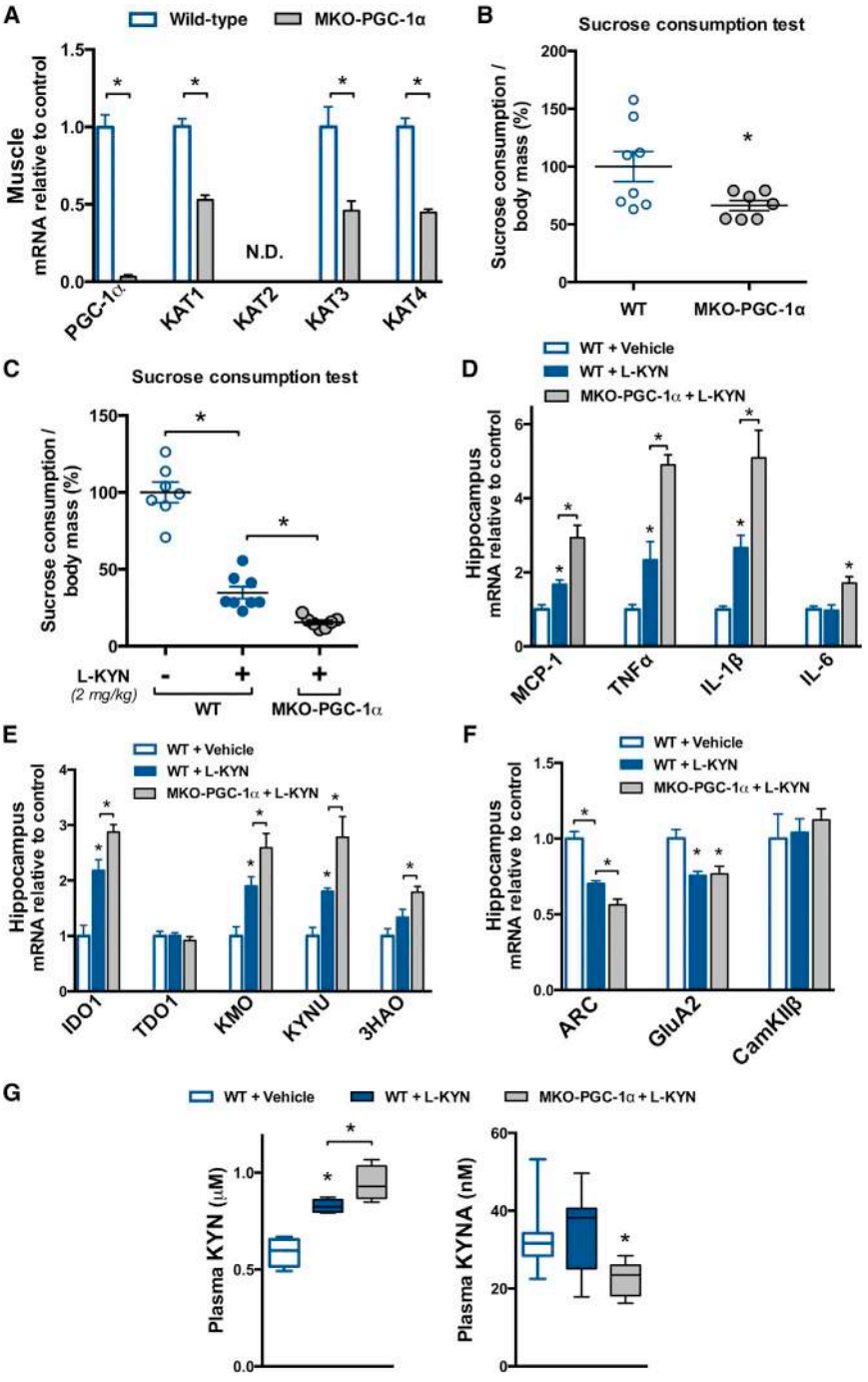

Figure 5. Skeletal Muscle-Specific PGC-1α Deletion Sensitizes to KYN-Induced Depressive Behavior

(A) mRNA levels in gastrocnemius muscle from WT and muscle-specific PGC-1α knockout mice (MKO-PGC-1α; n = 4–6).

(B) Sucrose consumption expressed as amount consumed normalized to body weight before KYN administration (SCT; n = 7–8).

(C) Sucrose consumption expressed as amount consumed normalized to body weight 2 hr after KYN administration in the same animals as in (B) (n = 7–8).

(D–F) Analysis of gene expression in hippocampus by qRT-PCR using primers specific to the indicated genes (n > 5).

(G) Plasma KYN and KYNA concentration shown as box plots (n = 5–7). Scale bars represent mean values and error bars represent SEM. N.D., not detectable. *p < 0.05.

See also Figure S5 and Table S3.

mck-PGC-1α1 animals had increased skeletal muscle PPARα and δ expression, which was further enhanced by CMS (Figure S6D). Treatment of WT myotubes with a selective PPARα agonist increased KAT1, KAT3, and KAT4 expression, while a selective PPARδ agonist affected only KAT1 levels (Figure S6E). PPAR ligand-mediated increase in KAT1 and KAT3 expression was strictly dependent on PGC-1α1, whereas KAT4 was still responsive to PPARα activation even in MKO-PGC-1α myotubes (Figure S6E). Combining PGC-1α1 expression with PPARα or δ activation resulted in the highest increase in KAT gene expression (Figure 6C). Conversely, reducing PPARα levels in myotubes resulted in decreased KAT levels, whereas silencing PPARδ expression affected only KAT1 (Figure 6D). This was verified also in the presence of overexpressed PGC-1α1 (Figure 6D). By using in vivo chromatin immunoprecipitation experiments we could confirm that, in mck-PGC-1α1 skeletal muscle, PPARα, PPARδ, and PGC-1α1 can be found associated with discrete regulatory regions upstream of the transcription start site of the KAT1, KAT3, and KAT4 genes (Figure 6E). These results suggest the PGC-1α1-PPARα/δ partnership is required for full effects on KAT gene expression in skeletal muscle in a cell-autonomous manner.

Exercise Training Increases Murine and Human KAT Expression in Skeletal Muscle

To verify if the PGC-1α1-KAT-KYN mechanism is part of the physiological response to exercise training, we analyzed WT mice after 8 weeks of free wheel running. This exercise intervention resulted in a gene expression profile that significantly overlapped with ectopic PGC-1α1 expression in skeletal muscle (Figure 7A). Notably, endurance exercise training increased skeletal muscle expression of KAT1, KAT3, and KAT4, decreased TDO1 and KMO expression (Figures 7A and S7A), and increased plasma KYNA levels (Figure 7B). Plasma KYNA levels directly correlated with murine skeletal muscle gene expression of KAT1, KAT3, and KAT4 (Figure S7B). We next determined the expression of

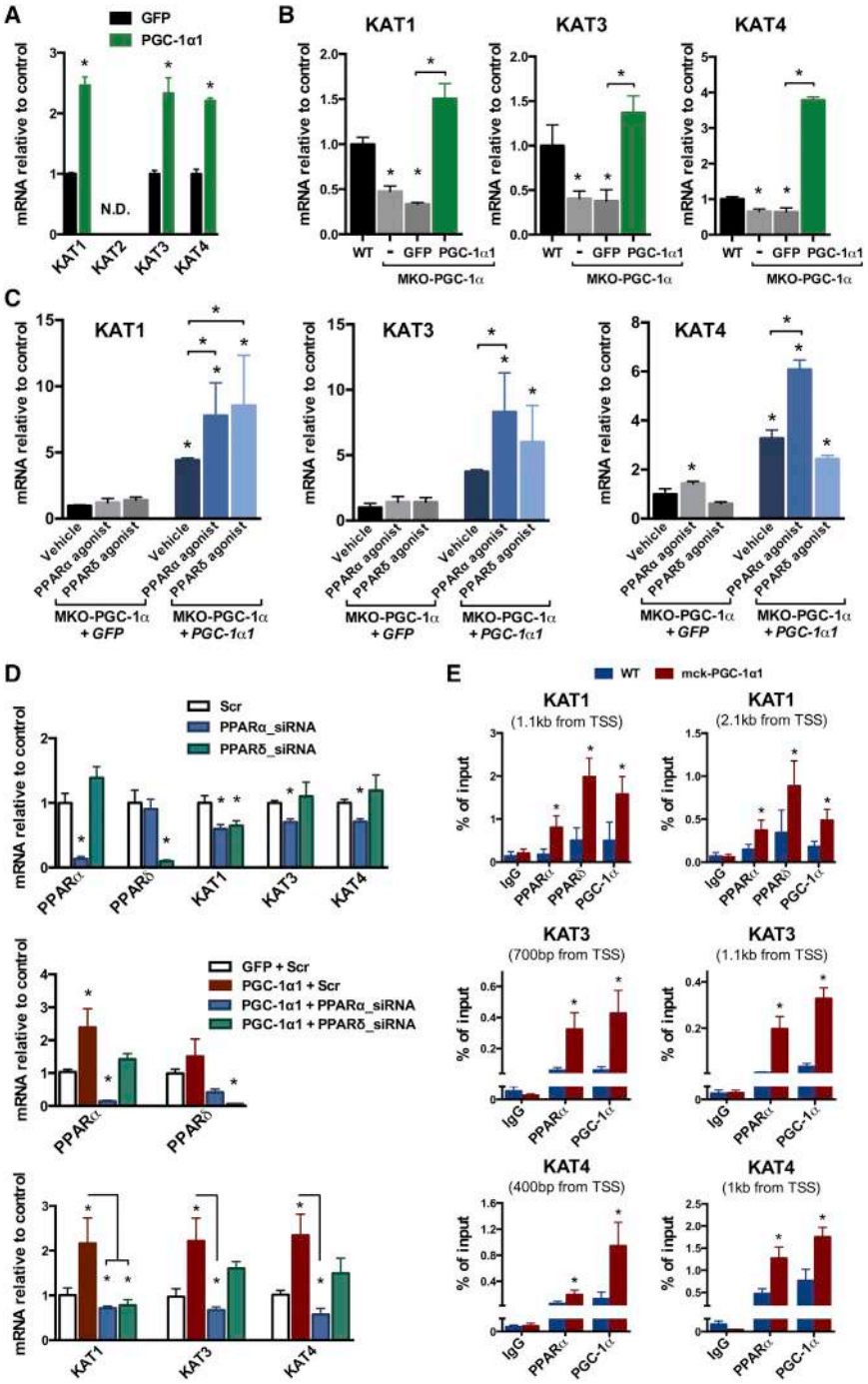

Figure 6. A PGC-1α1-PPARα/δ Partnership Regulates Myotube KATs Expression

(A and B) KAT mRNA levels in primary myotubes from WT or MKO-PGC-1α mice transduced with adenovirus expressing GFP alone or together with PGC-1α1 (n = 3).

(C) KAT mRNA levels in MKO-PGC-1α myotubes treated with vehicle, or selective PPARα or PPARδ agonists upon GFP or PGC-1α1 expression (n = 3).

(D) mRNA levels in myotubes from WT mice treated with siRNA for PPARα or PPARδ (n = 3), transduced as in (A).

(E) In vivo chromatin immunoprecipitation of PPARα-, PPARδ-, and PGC-1α1-associated DNA regions in skeletal muscle of WT and mck-PGC-1α1 animals (n = 4–6), shows occupancy of KAT gene regulatory region containing PPRE motifs. Scale bars represent mean values and error bars represent SD. N.D., not detectable. *p < 0.05. Transcription start site (TSS).

See also Figure S6 and Table S3.

KATs in human skeletal muscle before and after a 3-week training program (Czepluch et al., 2011). Percutaneous biopsies of the *vastus lateralis* skeletal muscle were obtained for each individual at baseline and 48 hr after the last training session. In agreement with previous reports (Mahoney and Tarnopolsky, 2005; Ruas et al., 2012; Schmitt et al., 2003), 3 weeks of physical exercise increased the expression of PGC-1α, PPARα, and PPARδ in human skeletal muscle (Figure 7C). Notably, the same individuals showed an increase in the expression levels of KAT1–KAT4 in skeletal muscle (Figure 7D), after the exercise training program (Figure 7E).

DISCUSSION

Many of the difficulties in treating depression stem from the considerable heterogeneity of the disease and a lack of defined etiology. Mechanisms suggested to contribute to depression include decrease in neurogenesis (Kheirbek et al., 2012), changes in levels of serotonin and other monoamines (Hirschfeld, 2000), neuroinflammation and astrocyte activation (Rajkowska and Miguel-Hidalgo, 2007), brain plasticity (Castrén, 2013), and glutamate imbalance (Sanacora et al., 2012). All of these aspects are affected by physical activity (Brené et al., 2007; Eyre and Baune, 2012), which has emerged as an important therapeutic alternative in affective disorders. In this study, we identify a mechanism by which skeletal muscle PGC-1α1 induced by exercise training changes tryptophan-kynurenine metabolism and protects from stress-induced depression. This mechanism is mediated by the actions of PGC-1α1 and the PPARα/δ transcription factors that together induce the expression of KAT enzymes, thus shifting peripheral KYN to KYNA.

Peripheral tryptophan conversion to KYN under proinflammatory and stress conditions is linked to neuroinflammation and considered to contribute to the pathogenesis of depression (Schwarcz et al., 2012). In this study, we observe a clear relationship between plasma KYN levels and expression of both inflammatory and synaptic proteins. Because KYNA, in contrast

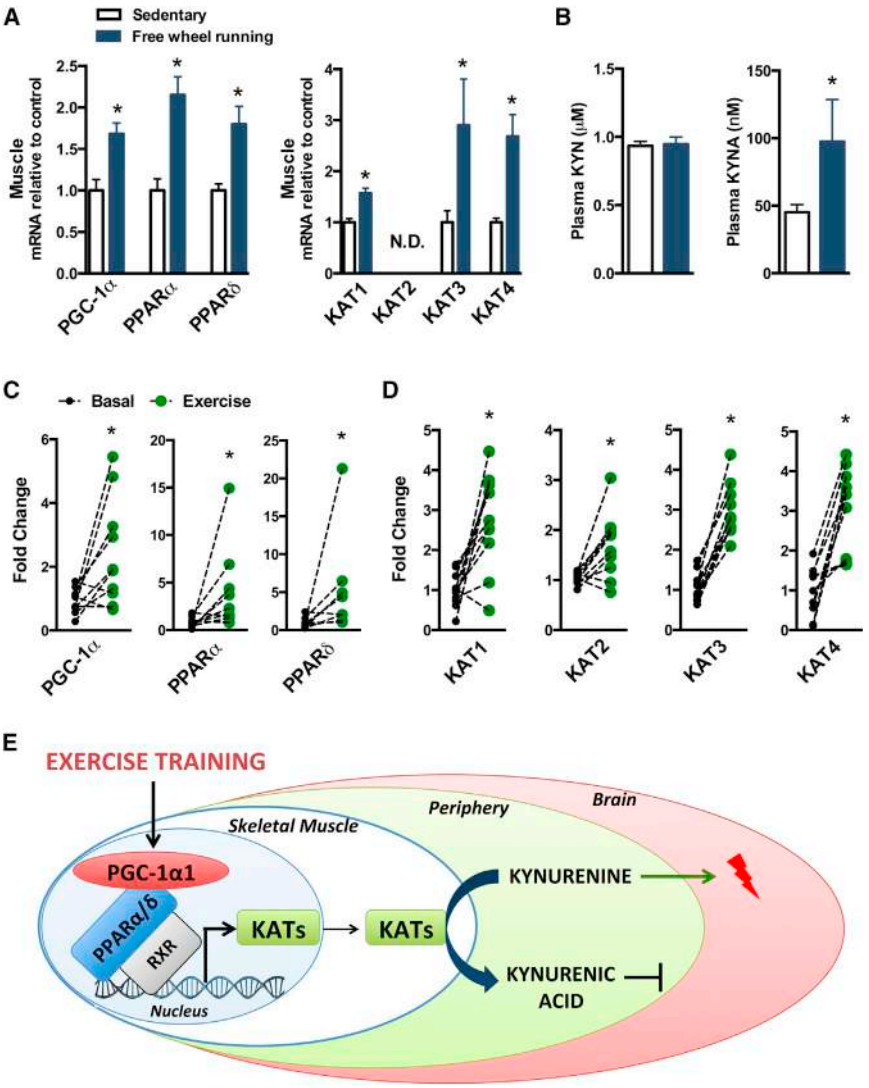

Figure 7. Exercise Training Increases Murine and Human KAT Expression in Skeletal Muscle

(A) Analysis of gene expression by qRT-PCR in gastrocnemius from sedentary and exercise-trained WT mice (n = 4–6).

(B) Plasma KYN and KYNA concentration (n = 6–8).

(C and D) Individual exercise training-induced changes in gene expression determined by qRT-PCR of *vastus lateralis* skeletal muscle from healthy volunteers (n = 8–10).

(E) Synoptic figure highlighting the molecular mechanism by which skeletal muscle PGC-1α1 shifts peripheral metabolism of KYN into KYNA. Scale bars represent mean values and error bars represent SEM. N.D., not detectable. *p < 0.05. See also Figure S7 and Table S3.

to KYN, does not pass the blood-brain barrier (Fukui et al., 1991), increased peripheral conversion of KYN to KYNA observed in the mck-PGC-1α1 mice should have a protective effect on the brain. Indeed, while the CMS treatment increases microglia and neuroinflammatory markers in WT mice, these changes do not occur in mkc-PGC-1α1 mice. In addition, synaptic proteins, as well as proteins mediating synaptic plasticity, are reduced by CMS in WT but not in mck-PGC-1α1 mice. However, this is not due to an overall protection from stress or stress-induced inflammation, as stressed mck-PGC1α1 mice display weight loss, increased skeletal muscle inflammatory markers, and higher CRH levels than unstressed transgenic mice.

The importance of the enhanced peripheral KYN breakdown is illustrated by the fact that mck-PGC-1α1 mice are protected from developing depressive behavior, even upon direct KYN administration. Conversely, MKO-PGC-1α mice display signs of depressive behavior at baseline, which worsens with KYN administration. The genetic loss of skeletal muscle PGC-1α impairs endurance performance in forced exercise tests (Handschin et al., 2007). This could be a confounding factor for behavioral analysis relying on motor activity such as forced swim tests, thus we used only the sucrose consumption test. Even so, we cannot exclude that the effect on sucrose consumption elicited by the KYN injections is due to sickness behavior rather than anhedonia per se (Dantzer et al., 2008). Nevertheless, this does not affect the conclusion that PGC-1α1-mediated regulation of skeletal muscle KAT levels and the consequent breaking down of KYN prevents a central response.

Diabetic and/or obese mice and humans have reduced PGC-1α levels in skeletal muscle, which has been suggested to lead or contribute to metabolic disease. In line with this, the link between insulin resistance, inflammation, and the kynurenine pathway is an emerging theme in recent literature (Oxenkrug, 2013). This is particularly evident in the context of aging (also associated with reduced muscle PGC-1α expression) (Johnson et al., 2013). Our results imply that dysregulation in the PGC-1α/kynurenine pathway could contribute to the increased risk for depression in type 2 diabetes patients (Roy and Lloyd, 2012; Stuart and Baune, 2012).

In general, the stress-induced molecular signature we observe in the brains of WT mice was not seen in mck-PGC-1α1 mice. The fact that the levels of astrocytic proteins EAAT1 and GFAP are affected by CMS supports the role of astrocytes in mediating stress-induced depression (Bajramović et al., 2000; Banasr et al., 2010; Bechtholt-Gompf et al., 2010; Czéh et al., 2006). Of note, some of the molecular pathways analyzed are already changed in brains of mck-PGC-1α1 mice at baseline, even without the CMS challenge. This suggests that other, not yet identified, signaling pathway(s) from skeletal muscle to brain might be active in mck-PGC-1α1 mice.

Skeletal muscle can act as an endocrine organ, secreting diverse myokines in a context-dependent manner (Brandt and Pedersen, 2010). One such myokine under PGC-1α1 control is cleaved from FNDC5 and secreted as Irisin, shown to impact adipose tissue function and systemic energy expenditure (Boström et al., 2012). It has been recently reported that peripheral FNDC5 delivery by viral vectors has a neuroprotective effect mediated by increased neuronal BDNF expression (Wrann et al., 2013). As previously reported, we observed that CMS induces a reduction in BDNF expression in WT mice (Gibney et al., 2013; Smith et al., 1995). However, BDNF levels remained unchanged in mck-PGC-1α1 mice, indicating that the FNDC5/BDNF pathway is unlikely to be a major component in the protection against stress-induced depression.

The use of PGC-1α genetic models allowed us to isolate skeletal muscle conditioning from other exercise components. The relevance of the proposed mechanism is supported by the fact that aerobic exercise training interventions in mice and humans induced skeletal muscle PGC-1α, PPARα/δ, and KAT expression. It will be interesting to expand this study design to a larger cohort of human volunteers, to include also patients with depression. The exercise training protocol used in this study was sufficient to increase plasma KYNA levels in rodents. In agreement with this, human plasma KYNA levels have been reported to increase after extensive endurance exercise (Lewis et al., 2010).

Depression is one of the world's leading causes of disease burden and time lived with disability (Whiteford et al., 2013) and current antidepressant treatments are insufficient (McClintock et al., 2011). By inducing exercise-mimetic changes specifically in skeletal muscle we have identified a mechanism that reduces the detrimental effects of stress and enhances the resilience to depression. Our work suggests that there is great therapeutic potential in targeting the PGC-1α1-PPARα/δ-KAT-Kynurenine pathway in depressive disorders (Schwarcz et al., 2012; Wu et al., 2014) thus harnessing one of the many beneficial effects of exercise training (Liu et al., 2013).

EXPERIMENTAL PROCEDURES

Please see the Extended Experimental Procedures for additional details.

Animal Experimentation

Mck-PGC-1α and MKO-PGC-1α animals (all on C57BL/6J background), a kind gift from Dr. Bruce Spiegelman (Harvard Medical School, Boston, MA), have been previously described (Chinsomboon et al., 2009; Lin et al., 2002). All experiments and protocols were approved by the regional animal ethics committee of Northern Stockholm.

Chronic Mild Stress

Male mice (8- to 10-week-old at the start of experiments) were subjected to stressors several times a day, applied at different time points to avoid habituation (Table S1). Behavioral testing was carried out 24 hr or more after the last stressor to evaluate depressive-like behavior.

Exercise Training

C57BL/6J male mice (9 weeks) were single housed with or without access to a running wheel for 8 weeks. Only mice that had run more than 4 km/night were selected for subsequent experiments.

Vastus lateralis skeletal muscle biopsies were obtained from healthy volunteers as previously described (Barrès et al., 2012). Muscle biopsies were obtained before training and 48 hr after the last exercise training session (Czepluch et al., 2011). All participants provided written informed consent and all protocols were approved by the Karolinska Institutet Ethics Committee (Czepluch et al., 2011).

Behavior

Forced Swim Test

Each mouse was placed in a cylinder containing 15 cm water for 15 min. After 24 hr, the animals were placed again in the cylinder and the duration of immobility (including movements to keep afloat, but not active swimming) was scored for a 5 min period.

Sucrose Consumption Test

Mice were individually housed, deprived of food for 6 hr, and water for 12 hr before the test, and then given access to 1% sucrose solution during 1 hr. The amount consumed was normalized to body weight. For L-Kynurenine treatments, 2 mg/kg of L-KYN (Sigma-Aldrich) or saline were injected intraperitoneally. Sucrose consumption was assessed 2 hr after injection.

Cell Culture

Primary myoblast cultures and adenovirus expressing PGC-1α1 or GFP (green fluorescent protein) have been previously described (Ruas et al., 2012). Fully differentiated myotubes were treated overnight with 1 μM CP775146 (PPARα agonist), or GW0742 (PPARδ agonist) (Tocris bioscience). Myoblasts were transfected with siRNA for PPARα and PPARδ and then differentiated.

Western Blot

Brain tissue samples were sonicated in RIPA-buffer with protease inhibitors. Muscle tissue was lysed in Isol-RNA lysis reagent (5 Prime). All primary antibodies used are listed in Table S2.

Chromatin Immunoprecipitation

Chromatin immunoprecipitation (ChIP) experiments were performed as previously described (Ruas et al., 2012) with some modifications.

Gene Expression Analysis

Total RNA was isolated using Isol-RNA Lysis Reagent (5 PRIME). Quantitative real-time PCR was performed and analysis of gene expression was performed using the ΔΔCt method. Primer sequences are listed in Table S3.

High-Performance Liquid Chromatography

Briefly, brain-tissue homogenate or plasma was analyzed for KYN, KYNA, and 3-HK levels using an isocratic reversed-phase high-performance liquid chromatography (HPLC) system.

Liquid Chromatography and Mass Spectrometry

Brain-tissue homogenate and plasma were prepared by ultracentrifugation and solid extraction and used for tryptophan and serotonin analysis by liquid chromatography-tandem mass spectrometry (LC-MS/MS).

Statistical Analysis

Data are expressed as average ± SD for in vitro and ± SEM for in vivo experiments. Statistical analyses were performed using GraphPad Prism 6. Unpaired Student's t test was used when two groups were compared, and one-way ANOVA followed by a protected Fisher's least significance difference (LSD) test for post hoc comparisons was used to compare multiple groups. Statistical significance was defined as $p < 0.05$. Correlations were calculated by Spearman rank correlation.

SUPPLEMENTAL INFORMATION

Supplemental Information includes Extended Experimental Procedures, seven figures, and three tables and can be found with this article at http://dx.doi.org/10.1016/j.cell.2014.07.051.

AUTHOR CONTRIBUTIONS

M.L. and J.L.R. conceptualized and supervised the study. L.Z.A. and T.F. contributed to the study design. L.Z.A., T.F., and M.L. performed and analyzed

behavior tests. L.Z.A. performed and analyzed tissue culture experiments, gene expression, and chromatin immunoprecipitations, with contributions from M.P.-P., V.M.-R., J.C.C., A.T.P., and D.M.S.F. T.F. performed and analyzed immunoblots. F.O., M.G., and S.E. performed and analyzed tryptophan and serotonin metabolite measurements. M.B. and I.S.-K. performed and analyzed tryptophan and serotonin measurements. A.K., R.B., and J.R.Z. performed the human exercise study and contributed muscle samples. A.K., J.R.Z., and S.E. edited the manuscript. L.Z.A., T.F., M.L., and J.L.R. wrote the manuscript.

ACKNOWLEDGMENTS

The authors would like to thank Karin Pernold for expert help with animal experiments. This project was supported by grants from the AstraZeneca-Karolinska Institutet Joint Research Program in Translational Science, Novo Nordisk Foundation (Denmark), Petrus and Augusta Hedlund's Foundation, Stockholm County Council, Strategic Research Programme in Diabetes at Karolinska Institutet, Swedish Brain Foundation, Swedish Diabetes Association, Swedish Foundation for Strategic Research, Swedish Research Council, Knut and Alice Wallenberg Foundation, Åhlen Foundation, and Åke Wiberg Foundation. F.O. is supported by a Karolinska Institutet doctoral fellowship. J.C.C. was supported in part by a PhD fellowship from the Fundação para a Ciência e Tecnologia (FCT, Portugal), V.M.R. and D.M.S.F. by postdoctoral fellowships from the Wenner-Gren Foundations (Sweden), and A.T.P. by a postdoctoral fellowship from the Swedish Society for Medical Research (SSMF).

Received: March 31, 2014
Revised: June 27, 2014
Accepted: July 16, 2014
Published: September 25, 2014

REFERENCES

Anisman, H., and Hayley, S. (2012). Inflammatory factors contribute to depression and its comorbid conditions. Sci. Signal. *5*, pe45.

Arany, Z. (2008). PGC-1 coactivators and skeletal muscle adaptations in health and disease. Curr. Opin. Genet. Dev. *18*, 426–434.

Baar, K., Wende, A.R., Jones, T.E., Marison, M., Nolte, L.A., Chen, M., Kelly, D.P., and Holloszy, J.O. (2002). Adaptations of skeletal muscle to exercise: rapid increase in the transcriptional coactivator PGC-1. FASEB J. *16*, 1879–1886.

Bajramović, J.J., Bsibsi, M., Geutskens, S.B., Hassankhan, R., Verhulst, K.C., Stege, G.J., de Groot, C.J., and van Noort, J.M. (2000). Differential expression of stress proteins in human adult astrocytes in response to cytokines. J. Neuroimmunol. *106*, 14–22.

Banasr, M., Chowdhury, G.M., Terwilliger, R., Newton, S.S., Duman, R.S., Behar, K.L., and Sanacora, G. (2010). Glial pathology in an animal model of depression: reversal of stress-induced cellular, metabolic and behavioral deficits by the glutamate-modulating drug riluzole. Mol. Psychiatry *15*, 501–511.

Barrès, R., Yan, J., Egan, B., Treebak, J.T., Rasmussen, M., Fritz, T., Caidahl, K., Krook, A., O'Gorman, D.J., and Zierath, J.R. (2012). Acute exercise remodels promoter methylation in human skeletal muscle. Cell Metab. *15*, 405–411.

Bechtholt-Gompf, A.J., Walther, H.V., Adams, M.A., Carlezon, W.A., Jr., Ongür, D., and Cohen, B.M. (2010). Blockade of astrocytic glutamate uptake in rats induces signs of anhedonia and impaired spatial memory. Neuropsychopharmacology *35*, 2049–2059.

Boström, P., Wu, J., Jedrychowski, M.P., Korde, A., Ye, L., Lo, J.C., Rasbach, K.A., Boström, E.A., Choi, J.H., Long, J.Z., et al. (2012). A PGC1-α-dependent myokine that drives brown-fat-like development of white fat and thermogenesis. Nature *481*, 463–468.

Brandt, C., and Pedersen, B.K. (2010). The role of exercise-induced myokines in muscle homeostasis and the defense against chronic diseases. J. Biomed. Biotechnol. *2010*, 520258.

Brené, S., Bjørnebekk, A., Åberg, E., Mathé, A.A., Olson, L., and Werme, M. (2007). Running is rewarding and antidepressive. Physiol. Behav. *92*, 136–140.

Castrén, E. (2013). Neuronal network plasticity and recovery from depression. JAMA Psychiatry *70*, 983–989.

Chinsomboon, J., Ruas, J., Gupta, R.K., Thom, R., Shoag, J., Rowe, G.C., Sawada, N., Raghuram, S., and Arany, Z. (2009). The transcriptional coactivator PGC-1alpha mediates exercise-induced angiogenesis in skeletal muscle. Proc. Natl. Acad. Sci. USA *106*, 21401–21406.

Choi, C.S., Befroy, D.E., Codella, R., Kim, S., Reznick, R.M., Hwang, Y.J., Liu, Z.X., Lee, H.Y., Distefano, A., Samuel, V.T., et al. (2008). Paradoxical effects of increased expression of PGC-1alpha on muscle mitochondrial function and insulin-stimulated muscle glucose metabolism. Proc. Natl. Acad. Sci. USA *105*, 19926–19931.

Claes, S., Myint, A.M., Domschke, K., Del-Favero, J., Entrich, K., Engelborghs, S., De Deyn, P., Mueller, N., Baune, B., and Rothermundt, M. (2011). The kynurenine pathway in major depression: haplotype analysis of three related functional candidate genes. Psychiatry Res. *188*, 355–360.

Czéh, B., Simon, M., Schmelting, B., Hiemke, C., and Fuchs, E. (2006). Astroglial plasticity in the hippocampus is affected by chronic psychosocial stress and concomitant fluoxetine treatment. Neuropsychopharmacology *31*, 1616–1626.

Czepluch, F.S., Barrès, R., Caidahl, K., Olieslagers, S., Krook, A., Rickenlund, A., Zierath, J.R., and Waltenberger, J. (2011). Strenuous physical exercise adversely affects monocyte chemotaxis. Thromb. Haemost. *105*, 122–130.

Dantzer, R., O'Connor, J.C., Freund, G.G., Johnson, R.W., and Kelley, K.W. (2008). From inflammation to sickness and depression: when the immune system subjugates the brain. Nat. Rev. Neurosci. *9*, 46–56.

Deussing, J.M., and Wurst, W. (2005). Dissecting the genetic effect of the CRH system on anxiety and stress-related behaviour. C. R. Biol. *328*, 199–212.

Duman, R.S., and Monteggia, L.M. (2006). A neurotrophic model for stress-related mood disorders. Biol. Psychiatry *59*, 1116–1127.

Duman, R.S., and Aghajanian, G.K. (2012). Synaptic dysfunction in depression: potential therapeutic targets. Science *338*, 68–72.

Eisele, P.S., Salatino, S., Sobek, J., Hottiger, M.O., and Handschin, C. (2013). The peroxisome proliferator-activated receptor γ coactivator 1α/β (PGC-1) coactivators repress the transcriptional activity of NF-κB in skeletal muscle cells. J. Biol. Chem. *288*, 2246–2260.

Eyre, H., and Baune, B.T. (2012). Neuroimmunological effects of physical exercise in depression. Brain Behav. Immun. *26*, 251–266.

Femenía, T., Gómez-Galán, M., Lindskog, M., and Magara, S. (2012). Dysfunctional hippocampal activity affects emotion and cognition in mood disorders. Brain Res. *1476*, 58–70.

Foy, M.R., Stanton, M.E., Levine, S., and Thompson, R.F. (1987). Behavioral stress impairs long-term potentiation in rodent hippocampus. Behav. Neural Biol. *48*, 138–149.

Froger, N., Palazzo, E., Boni, C., Hanoun, N., Saurini, F., Joubert, C., Dutriez-Casteloot, I., Enache, M., Maccari, S., Barden, N., et al. (2004). Neurochemical and behavioral alterations in glucocorticoid receptor-impaired transgenic mice after chronic mild stress. J. Neurosci. *24*, 2787–2796.

Fukui, S., Schwarcz, R., Rapoport, S.I., Takada, Y., and Smith, Q.R. (1991). Blood-brain barrier transport of kynurenines: implications for brain synthesis and metabolism. J. Neurochem. *56*, 2007–2017.

Gál, E.M., and Sherman, A.D. (1980). L-kynurenine: its synthesis and possible regulatory function in brain. Neurochem. Res. *5*, 223–239.

Gibb, J., Hayley, S., Poulter, M.O., and Anisman, H. (2011). Effects of stressors and immune activating agents on peripheral and central cytokines in mouse strains that differ in stressor responsivity. Brain Behav. Immun. *25*, 468–482.

Gibney, S.M., McGuinness, B., Prendergast, C., Harkin, A., and Connor, T.J. (2013). Poly I:C-induced activation of the immune response is accompanied by depression and anxiety-like behaviours, kynurenine pathway activation and reduced BDNF expression. Brain Behav. Immun. *28*, 170–181.

Gómez-Galán, M., De Bundel, D., Van Eeckhaut, A., Smolders, I., and Lindskog, M. (2013). Dysfunctional astrocytic regulation of glutamate transmission in a rat model of depression. Mol. Psychiatry *18*, 582–594.

Han, Q., Cai, T., Tagle, D.A., and Li, J. (2010). Thermal stability, pH dependence and inhibition of four murine kynurenine aminotransferases. BMC Biochem. *11*, 19.

Handschin, C., Chin, S., Li, P., Liu, F., Maratos-Flier, E., Lebrasseur, N.K., Yan, Z., and Spiegelman, B.M. (2007). Skeletal muscle fiber-type switching, exercise intolerance, and myopathy in PGC-1alpha muscle-specific knock-out animals. J. Biol. Chem. *282*, 30014–30021.

Hirschfeld, R.M. (2000). History and evolution of the monoamine hypothesis of depression. J. Clin. Psychiatry *61* (*Suppl 6*), 4–6.

Johnson, M.L., Robinson, M.M., and Nair, K.S. (2013). Skeletal muscle aging and the mitochondrion. Trends Endocrinol. Metab. *24*, 247–256.

Kang, H.J., Voleti, B., Hajszan, T., Rajkowska, G., Stockmeier, C.A., Licznerski, P., Lepack, A., Majik, M.S., Jeong, L.S., Banasr, M., et al. (2012). Decreased expression of synapse-related genes and loss of synapses in major depressive disorder. Nat. Med. *18*, 1413–1417.

Kheirbek, M.A., Klemenhagen, K.C., Sahay, A., and Hen, R. (2012). Neurogenesis and generalization: a new approach to stratify and treat anxiety disorders. Nat. Neurosci. *15*, 1613–1620.

Lawlor, D.A., and Hopker, S.W. (2001). The effectiveness of exercise as an intervention in the management of depression: systematic review and meta-regression analysis of randomised controlled trials. BMJ *322*, 763–767.

Lewis, G.D., Farrell, L., Wood, M.J., Martinovic, M., Arany, Z., Rowe, G.C., Souza, A., Cheng, S., McCabe, E.L., Yang, E., et al. (2010). Metabolic signatures of exercise in human plasma. Sci. Transl. Med. *2*, 33ra37.

Lin, J., Wu, H., Tarr, P.T., Zhang, C.Y., Wu, Z., Boss, O., Michael, L.F., Puigserver, P., Isotani, E., Olson, E.N., et al. (2002). Transcriptional co-activator PGC-1 alpha drives the formation of slow-twitch muscle fibres. Nature *418*, 797–801.

Lin, J., Handschin, C., and Spiegelman, B.M. (2005). Metabolic control through the PGC-1 family of transcription coactivators. Cell Metab. *1*, 361–370.

Liu, W., Sheng, H., Xu, Y., Liu, Y., Lu, J., and Ni, X. (2013). Swimming exercise ameliorates depression-like behavior in chronically stressed rats: relevant to proinflammatory cytokines and IDO activation. Behav. Brain Res. *242*, 110–116.

Lloyd, R.B., and Nemeroff, C.B. (2011). The role of corticotropin-releasing hormone in the pathophysiology of depression: therapeutic implications. Curr. Top. Med. Chem. *11*, 609–617.

Mahoney, D.J., and Tarnopolsky, M.A. (2005). Understanding skeletal muscle adaptation to exercise training in humans: contributions from microarray studies. Phys. Med. Rehabil. Clin. N. Am. *16*, 859–873, vii.

McClintock, S.M., Husain, M.M., Wisniewski, S.R., Nierenberg, A.A., Stewart, J.W., Trivedi, M.H., Cook, I., Morris, D., Warden, D., and Rush, A.J. (2011). Residual symptoms in depressed outpatients who respond by 50% but do not remit to antidepressant medication. J. Clin. Psychopharmacol. *31*, 180–186.

McNally, L., Bhagwagar, Z., and Hannestad, J. (2008). Inflammation, glutamate, and glia in depression: a literature review. CNS Spectr. *13*, 501–510.

Melanie, C., Nicola, J.W., John, C., Sandra, P.H., Anne, M.H., Adrian, H.T., Kenneth, R.F., Ceire, C., Aidan, S., Helen, B., et al. (2012). Facilitated physical activity as a treatment for depressed adults: randomised controlled trial. BMJ *344*, e2758.

Müller, N., and Schwarz, M.J. (2007). The immune-mediated alteration of serotonin and glutamate: towards an integrated view of depression. Mol. Psychiatry *12*, 988–1000.

Myint, A.-M., and Kim, Y.-K. (2014). Network beyond IDO in psychiatric disorders: revisiting neurodegeneration hypothesis. Prog. Neuropsychopharmacol. Biol. Psychiatry *48*, 304–313.

Oxenkrug, G. (2013). Insulin resistance and dysregulation of tryptophan-kynurenine and kynurenine-nicotinamide adenine dinucleotide metabolic pathways. Mol. Neurobiol. *48*, 294–301.

Pittenger, C. (2013). Disorders of memory and plasticity in psychiatric disease. Dialogues Clin. Neurosci. *15*, 455–463.

Rajkowska, G., and Miguel-Hidalgo, J.J. (2007). Gliogenesis and glial pathology in depression. CNS Neurol. Disord. Drug Targets *6*, 219–233.

Roy, T., and Lloyd, C.E. (2012). Epidemiology of depression and diabetes: a systematic review. J. Affect. Disord. Suppl. *142*, S8–S21.

Ruas, J.L., White, J.P., Rao, R.R., Kleiner, S., Brannan, K.T., Harrison, B.C., Greene, N.P., Wu, J., Estall, J.L., Irving, B.A., et al. (2012). A PGC-1α isoform induced by resistance training regulates skeletal muscle hypertrophy. Cell *151*, 1319–1331.

Sanacora, G., Treccani, G., and Popoli, M. (2012). Towards a glutamate hypothesis of depression: an emerging frontier of neuropsychopharmacology for mood disorders. Neuropharmacology *62*, 63–77.

Schmitt, B., Flück, M., Décombaz, J., Kreis, R., Boesch, C., Wittwer, M., Graber, F., Vogt, M., Howald, H., and Hoppeler, H. (2003). Transcriptional adaptations of lipid metabolism in tibialis anterior muscle of endurance-trained athletes. Physiol. Genomics *15*, 148–157.

Schwarcz, R., Bruno, J.P., Muchowski, P.J., and Wu, H.Q. (2012). Kynurenines in the mammalian brain: when physiology meets pathology. Nat. Rev. Neurosci. *13*, 465–477.

Short, K.R., Vittone, J.L., Bigelow, M.L., Proctor, D.N., Rizza, R.A., Coenen-Schimke, J.M., and Nair, K.S. (2003). Impact of aerobic exercise training on age-related changes in insulin sensitivity and muscle oxidative capacity. Diabetes *52*, 1888–1896.

Smith, M.A., Makino, S., Kvetnansky, R., and Post, R.M. (1995). Stress and glucocorticoids affect the expression of brain-derived neurotrophic factor and neurotrophin-3 mRNAs in the hippocampus. J. Neurosci. *15*, 1768–1777.

Stuart, M.J., and Baune, B.T. (2012). Depression and type 2 diabetes: inflammatory mechanisms of a psychoneuroendocrine co-morbidity. Neurosci. Biobehav. Rev. *36*, 658–676.

Tochigi, M., Iwamoto, K., Bundo, M., Sasaki, T., Kato, N., and Kato, T. (2008). Gene expression profiling of major depression and suicide in the prefrontal cortex of postmortem brains. Neurosci. Res. *60*, 184–191.

Wang, Y.X., Zhang, C.L., Yu, R.T., Cho, H.K., Nelson, M.C., Bayuga-Ocampo, C.R., Ham, J., Kang, H., and Evans, R.M. (2004). Regulation of muscle fiber type and running endurance by PPARdelta. PLoS Biol. *2*, e294.

Whiteford, H.A., Degenhardt, L., Rehm, J., Baxter, A.J., Ferrari, A.J., Erskine, H.E., Charlson, F.J., Norman, R.E., Flaxman, A.D., Johns, N., et al. (2013). Global burden of disease attributable to mental and substance use disorders: findings from the Global Burden of Disease Study 2010. Lancet *382*, 1575–1586.

Willner, P. (2005). Chronic mild stress (CMS) revisited: consistency and behavioural-neurobiological concordance in the effects of CMS. Neuropsychobiology *52*, 90–110.

Wrann, C.D., White, J.P., Salogiannnis, J., Laznik-Bogoslavski, D., Wu, J., Ma, D., Lin, J.D., Greenberg, M.E., and Spiegelman, B.M. (2013). Exercise induces hippocampal BDNF through a PGC-1α/FNDC5 pathway. Cell Metab. *18*, 649–659.

Wu, H.Q., Okuyama, M., Kajii, Y., Pocivavsek, A., Bruno, J.P., and Schwarcz, R. (2014). Targeting kynurenine aminotransferase II in psychiatric diseases: promising effects of an orally active enzyme inhibitor. Schizophr. Bull. *40* (*Suppl 2*), S152–S158.

Yuen, E.Y., Wei, J., Liu, W., Zhong, P., Li, X., and Yan, Z. (2012). Repeated stress causes cognitive impairment by suppressing glutamate receptor expression and function in prefrontal cortex. Neuron *73*, 962–977.

Cell

EXTENDED EXPERIMENTAL PROCEDURES

Mice were housed in plastic cages (3-5 per cage) at 24 ± 1°C, 12/12 hr controlled light conditions with *ad-libitum* access to water and food (R34 Chow, Lantmänen, Sweden), unless indicated. All experiments were approved by the Ethical Committee of Northern Stockholm, Sweden. Experimenters were blinded to the experimental groups during behavioral experiments and assessments. Mck-PGC-1α1 transgenic and muscle-specific PGC-1α knockout mice (both on C57BL6/J background) have been previously described (Chinsomboon et al., 2009; Lin et al., 2002) and were bred in-house. Wild-type mice (C57BL/6J) were procured from Charles River (Germany).

Chronic Mild Stress

Wild-type (C57BL/6J) and mcK-PGC-1α1 transgenic mice (8-10-weeks-old, at the beginning of the experiment) were subjected to chronic mild stress (CMS) for a period of 5 weeks (García-Gutiérrez et al., 2010; Willner, 2005) to induce depressive-like behavior. The corresponding controls (n = 8-10/group) were kept in the usual housing conditions without stress, and routine handling was carried out to minimize stress during behavioral testing. Mice were subjected to one or more of the following stressors at unpredictable times during the day: wet cage, food deprivation, restraint, period of strobe light, reversal of light-dark cycle, cage tilting (45°) and loud noise (90–105 db) (see Table S1). All stressors and/or sequences were applied at different time points to avoid habituation and to add an element of unpredictability (García-Gutiérrez et al., 2010). Both control and stressed animals were weighed before CMS and twice per week after the first week of the CMS. 24 hr after the last stressor, animals were subjected to a forced swim test, 48 hr after this to the sucrose consumption test, and 72 hr later novel cage.

Behavior

Forced Swim Test

The FST has been used as a predictive model of depressive behavior (Porsolt et al., 1977). Briefly, each mouse was placed for 15 min in a vertical Plexiglas cylinder (height 25 cm diameter 18 cm) containing 15 cm water at 25+-1°C (Cryan et al., 2002). After 24 hr, the animals were placed again in the cylinder for 5 min and filmed. Films were used to score immobility time as an indication of behavioral despair. Floating movements, but not active swimming, were considered as immobility.

Sucrose Consumption Test

To examine anhedonia, a core symptom of depressive-like behavior, sucrose intake was assessed. Animals were deprived of water 12 hr before test, and food 6 hr before. Animals were weighed and put in individual cages with one drinking bottle with 1% sucrose solution. Amount of sucrose consumed was measured by weighing water bottles before and after the 1 hr session. Bottle weight difference was normalized to body weight per mouse and presented as the percentage of sucrose consumed per gram of body weight relative to control.

Sucrose Preference

Mice were habituated for 2 days to a 1% sucrose solution. The drinking bottles were switched of position every 24 hr to avoid location preference. After the habituation the consumption of both water and sucrose were measured for 24h and expressed as sucrose intake/total intake*100.

Novel Cage

Mice were individually placed in a regular rectangular cage with bedding (35cmx25cm) after the CMS and filmed for 5 min to evaluate the individual behavior in a novel situation. The experiment was carried out during the dark/active phase of the rodents (from 20.00h-00.00 h). Parameters of activity were analyzed to evaluate the locomotion: % activity (time moving/total time*100), speed (cm/s) and distance traveled (cm). The individual tracking were analyzed with Ethovision XT 10 (Noldus, The Netherlands).

Exercise Training

Nine-week-old C57BL/6J male mice were single-housed and divided into 2 groups: control and exercise. After an acclimation period of 5-6 days the exercised group was given access to a running wheel with a counter that monitored revolutions during 8 weeks. Control group mice were housed in similar cages without running wheels. Only animals that had run more than 4 km/night were selected for subsequent experiments.

L-Kynurenine Treatment

L-Kynurenine sulfate salt (Sigma-Aldrich) was dissolved in sterile deionized water (pH 8.1-9) to a concentration of 0.5 mg/ml. Two mg/kg of L-KYN were injected intraperitoneal to 8 to 16-week-old mice that had been deprived of water during 8 hr. The control group received sterile saline injections. After the injections, mice were housed individually for 2 hr followed by assessment of sucrose consumption (1hr). Mice were sacrificed and tissues were harvested and snap-frozen in liquid nitrogen.

Cell Culture

Primary mouse myoblasts were isolated either from C57BL6/J or MKO-PGC-1α mice as previously described (Megeney et al., 1996). Myoblasts were cultured in F-10 medium (Invitrogen) supplemented with 20% FBS (Sigma-Aldrich), 5% penicillin streptomycin, and

basic FGF (both Invitrogen). To induce differentiation into myotubes, cells were shifted to DMEM media supplemented with 5% horse serum and 5% penicillin streptomycin (all Invitrogen).

Adenovirus-Mediated Expression

Recombinant adenovirus expressing mouse PGC-1α1 or GFP (green fluorescent protein) have been previously described (Ruas et al., 2012).

Cell Treatments

Differentiated wild-type myotubes and/or MKO-PGC-1α myotubes transduced with adenovirus were treated overnight with 1 μM of a selective PPARα agonist CP775146, and a selective PPARδ agonist GW0742 (both Tocris bioscience). Undifferentiated myotubes were transfected using lipofectamine RNAMax (life technologies) with siRNA for PPARα (Applied biosystems Lot# ASO0YL47) or with siRNA for PPARδ (Applied biosystems Lot# ASO0YL48). Cells were then differentiated and processed for analysis of gene expression, or transduced with the appropriate viral vector (as indicated).

Brain Microdissection

48 hr after the last behavioral test male mice were decapitated and brains were rapidly removed, fresh frozen and stored immediately at −80°C until use. Brains were cut in 500 μm slices with a cryostat, and dissected as previously described (Palkovits, 1983). Specific punchers from different sizes (0.75-2 mm, Harris UniCore, Ted Pella, Inc, Redding, California) were used to microdissect medial prefrontal cortex, cingulate cortex, nucleus accumbens, hypothalamus, hippocampus and amygdala. Anatomic regions were identified according to Paxinos and Watson (1998).

Western Blot

Hippocampal samples from one hemisphere were sonicated in RIPA-buffer (containing 1% Triton X-100, 0.1% SDS, 50 mM Tris-HCl pH7.5, 150 mM NaCl, 0.5% sodium deoxycolate and H2O) with a protease inhibitor (1:10 from Roche #04693124001). The samples were centrifuged at 14.000 rpm during 10 min at 4°C and supernatant was kept for protein analyses. BCA colorimetric method was used to determine the total amount of protein. Equal amounts of protein (30 μg) were loaded onto a NuPAGE 4%–12% Bis-Tris gel, Novex (Life Technologies, Glasgow, UK) and transferred to PVDF membranes (0.45 μm) Immobilon-FL (Millipore, Temecula, CA, USA). Detection was based on a fluorescent secondary antibody that was visualized using the LICOR (Lincoln, NE, USA) Odyssey infrared fluorescence detection system. The data were quantified using ImageJ software (NIH, Bethesda, MD, USA) normalizing the values with β-Actin or vinculin.

Muscle tissue was lysed in Isol-RNA lysis reagent (5 Prime) and total protein was extracted according to manufacturer's instructions. Protein concentration was determined by Bradford Protein Assay following manufacturer's instructions (BioRad). 60 μg of proteins were separated by SDS polyacrylamide gel membranes (PAGE) and transferred to PVDF membranes. After blocking with 10% skim milk, blots were incubated overnight at 4°C or 1h at room temperature with primary antibodies diluted in 0.1% bovine serum albumin (BSA). After washing, membranes were incubated with horseradish-peroxidase-conjugated secondary antibodies for 1h at room temperature. Blots were visualized by enhanced chemiluminiscence (GE Healthcare) and exposed on films. Quantification was performed using ImageJ software (NIH, Bethesda, MD, USA) normalizing the values with β-Actin. For primary antibodies see Table S2.

Analysis of Gene Expression

Total RNA was isolated from cells or tissues using Isol-RNA Lysis Reagent (5 PRIME) according to manufacturer's intructions. Afterward, 1 μg of RNA was treated with Amplification Grade DNase I (Life Technologies) and from that, 500 ng were used for cDNA preparation using the Applied Biosystem Reverse Transcription Kit (Life Technologies). Quantitative Real-Time PCR was performed in a ViiA 7 Real-Time PCR system thermal cycler with SYBR Green PCR Master Mix (both Applied Biosystems). Analysis of gene expression was performed using the ΔΔCt method and relative gene expression was normalized to hypoxanthine phosphoribosyltransferase (HPRT) mRNA levels. Gene expression analyses were expressed as mRNA levels relative to controls. Primer sequences are listed in Table S3.

Chromatin Immunoprecipitation

ChIP experiments were performed as previously described (Ruas et al., 2012) with the following modifications: 50 mg of skeletal muscle (gastrocnemius) was used per animal. Tissue was homogenized in PBS and crosslinked with 1% formaldehyde for 10 min. Glycine (125 mM) was added, followed by centrifugation at 4000 rpm for 5 min. After aspirating the supernatant, pellet was washed with 1 ml cold PBS followed by centrifugation at 4000 rpm for 5 min. This step was repeated with buffer 1 (0.25% Triton X-100, 10mM EDTA, 0.5mM EGTA, 10mM HEPES, pH 6.5) and buffer 2 (200mM NaCl, 1mM EDTA, 0.5mM EGTA, 10mM HEPES, pH 6.5). The pellet was then resuspended in 300 μl lysis buffer (1% SDS, 10mM EDTA, 50mM Tris-HCl, 1X protease cocktail inhibitor, pH 8). Afterward, samples were sonicated on ice using a Bioruptor (Diagenode) 40 times for 30 s ON and 30 s OFF.

High-Performance Liquid Chromatography

At the day of analysis, plasma was diluted (1:2, v/v), and brain tissue (1:5, w/v) with 0.4 M perchloric acid (PCA) (containing 0.1% sodium metabisulfite, 0.05% EDTA), and homogenized using an electrical disperser (T10 basic Ultra-Turrax, IKA Werke GmbH & Co. KG. Staufen, Germany). The homogenate was then centrifuged at 21000 × g for 5 min and the resulting supernatant was further diluted (1:1,10, v/v) by the addition of 70% strength PCA. This solution was then re-centrifuged (21000 × g, 5 min), and the supernatant transferred to a new eppendorf tube for analysis. To determine KYNA and kynurenine levels, samples were subjected to analysis utilizing an isocratic high performance reversed-phase liquid chromatography (HPLC) system, including a dual-piston, high-pressure delivery pump (Bishoff, Leonberg, Germany) and a ReproSil-Pur C18 column (4 × 150 mm, Dr. Maisch GmbH, Ammerbuch, Germany). A fluorescence detector (Jasco FP-2020, Hachioji City, Japan) with an excitation wavelength of 344 nm and an emission wavelength of 398 nm (18 nm bandwidth) was used for KYNA analyzis and a UV-VIS detector (SPD-10A, Shimadzu, Japan) operated at 365 nm for kynurenine analyzes. For detection of both KYNA and kynurenine, a mobile phase containing 50 mM sodium acetate and 7.0% acetonitrile in ultrapure dH_20 (pH 6.20 adjusted with acetic acid), was pumped through the column at a flow rate of 0.5 ml/ min. Samples (30 – 40 μl) were manually injected into a Rheodyne injector (Rhonert Park, CA) with a single sample loop volume of 100 μl (Cotati, CA). A second buffer containing zinc acetate (0.5 M not pH adjusted) was delivered postcolumnar by a peristaltic pump (P- 500 Pharmacia, Uppsala, Sweden) at a flow rate of 10 ml/hr. The signals from the fluorescence and UV-VIS detectors were transferred to a computer and analyzed by Datalys Azur Software (Grenoble, France). The retention times of KYNA and kynurenine were ≈7, and 4 min, respectively.

To determine 3-hydroxykynurenine (3HK) concentrations, samples were subjected to analysis utilizing an isocratic reversed-phase HPLC system coupled to an electrochemical detector (Coulochem III; ESA Inc.). A mobile phase consisting of 20 mM sodium phosphate, 0.7 mM octanesulfonic acid and 8% acetonitrile (pH set to 3.2 using acetic acid) was pumped through a Reprosil-Pur C18 column (4 × 150 mm, Dr. Maisch GmbH), at a flow rate of 0.6 ml/min, delivered by a LC-10AD VP (Shimadzu Corporation). Signals from the detector were transferred to a computer for analysis with Clarity (Data Apex Ltd, The Czech Republic). The retention time of 3HK was about 5 min.

Liquid Chromatography and Mass Spectrometry

Brain samples were weighed, homogenized in 600μL PBS buffer and ultracentrifuged at 4°C and 30000 g. The supernatant (50μL) was then added Internal Standard and prepared using solid phase extraction (Oasis® MAX). Mouse plasma and standard samples (50μL) were prepared using solid phase extraction (Oasis® MAX). D5-TRP and D4-SER was used as Internal Standard (IS, Sigma Aldrich). After solid phase extraction the brain, plasma and standard sample eluate were evaporated with nitrogen at 50°C and redissolved in 0.1% formic acid in MilliQ water. 7.5 μl of the filtrate was injected using a Waters Acquity HPLC system equipped with a HSST3 2.1 × 100mm, 1.8μm particle column. The detection was performed using a Waters Xevo TQ-S triple quadrupole mass spectrometer operating in positive ionization MS/MS configuration. The mobile phase was run at a flow rate of 300 μL/minute and consisted of 0.1% formic acid in MilliQ water (A phase) and 95% acetonitrile 0.1% formic acid (B phase) starting with 2% B for 2 min following gradient elution, total run time of 15 min. The formic acid and acetonitrile were purchased as MS-grade from Sigma-Aldrich. The mass spectrometer was tuned for TRP and SER and set at capillary voltage of 0.6kV, source temperature 150°C, desolvation temperature 500°C and desolvation gas flow of 500 L/h. The cone voltage was 10V and 12V, collision energy 26 and 34 eV for SER and TRP respectively. Mass spectral transition for TRP and SER was m/z 205 > 91, 177 > 115 and for the IS 210 > 150 and 181 > 118.

Quantification

Seven concentration standards of TRP and SER were used to establish a linear calibration curve and plotted using the ratio of analyte peak area over IS peak area after integration by Masslynx 4.1 software (Waters Corporation). Retention times for SER and TRP were 3.7 and 5.1 min respectively.

SUPPLEMENTAL REFERENCES

Cryan, J.F., Markou, A., and Lucki, I. (2002). Assessing antidepressant activity in rodents: recent developments and future needs. Trends Pharmacol. Sci. *23*, 238–245.

García-Gutiérrez, M.S., Pérez-Ortiz, J.M., Gutiérrez-Adán, A., and Manzanares, J. (2010). Depression-resistant endophenotype in mice overexpressing cannabinoid CB(2) receptors. Br. J. Pharmacol. *160*, 1773–1784.

Megeney, L.A., Perry, R.L., LeCouter, J.E., and Rudnicki, M.A. (1996). bFGF and LIF signaling activates STAT3 in proliferating myoblasts. Dev. Genet. *19*, 139–145.

Palkovits, M. (1983). Punch sampling biopsy technique. Methods Enzymol. *103*, 368–376.

Paxinos, G., and Watson, C. (1998). The Rat Brain in Stereotaxic Coordinates, Fourth Edition (Waltham, MA: Academic Press).

Porsolt, R.D., Le Pichon, M., and Jalfre, M. (1977). Depression: a new animal model sensitive to antidepressant treatments. Nature *266*, 730–732.

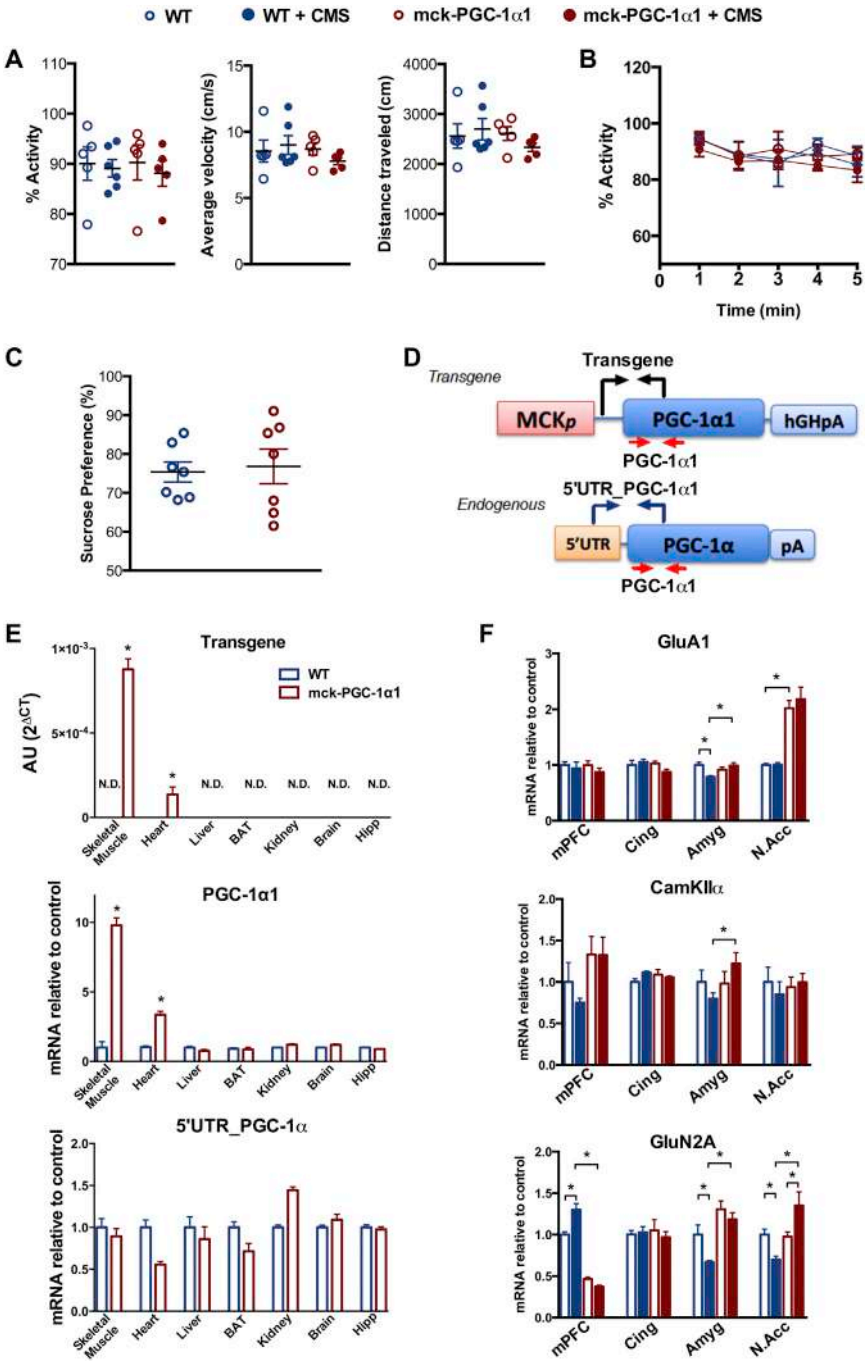

Figure S1. Muscle-Specific PGC-1α1 Transgene Expression, Related to Figure 1

(A and B) Measurement of parameters for locomotor activity during the novel cage test (n = 5).

(C) Sucrose preference of the indicated groups (n = 7).

(D) Schematic representation of the PGC-1α1 transgene driven by muscle creatine kinase promoter (MCKp) and followed by the human Growth Hormone polyA sequence (hGHpA). Arrows indicate different primer sets designed to detect total (red arrows), endogenous (blue arrows), and exogenous (black arrows) PGC-1α1 expression levels.

(E) PGC-1α1 expression levels in skeletal muscle, heart, liver, brown adipose tissue (BAT), kidney, brain, and isolated hippocampus were assessed by qRT-PCR using primers as described in (D) (n = 6).

(F) Analysis of gene expression in medial prefrontal cortex (mPFC), cingulate cortex (Cing), amygdala (Amyg), and nucleus accumbens (N.Acc) by qRT-PCR using primers specific to the indicated genes (n = 5-8). Bars depict mean values and error bars indicate SEM N.D. Not Detectable, AU arbitrary units, *p < 0.05.

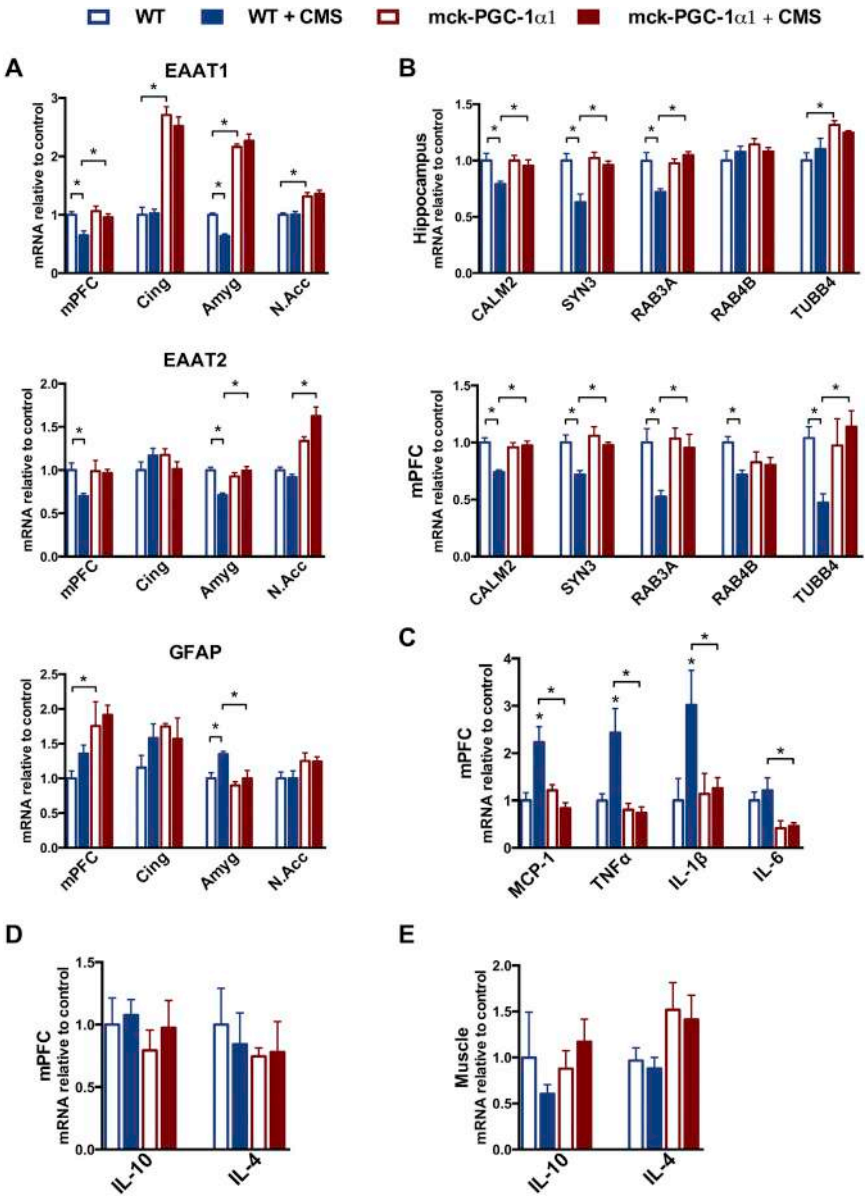

Figure S2. Chronic Mild Stress-Mediated Effects on Astrocytic, Synaptic, and Inflammatory Markers, Related to Figure 2

(A) Analysis of gene expression in medial prefrontal cortex (mPFC), cingulate cortex (Cing), amygdala (Amyg), and nucleus accumbens (N.Acc) by qRT-PCR using primers specific to the indicated genes (n = 5-8).

(B) Analysis of gene expression of synapse-related genes in hippocampus and medial prefrontal cortex (mPFC) from wild-type and mck-PGC-1α1 with and without chronic mild stress.

(C–E) qRT-PCR gene expression analysis of inflammatory (C) and anti-inflammatory cytokines in mPFC (D) and skeletal muscle (E) (n = 5-8). Bars depict mean values and error bars indicate SEM. *p < 0.05.

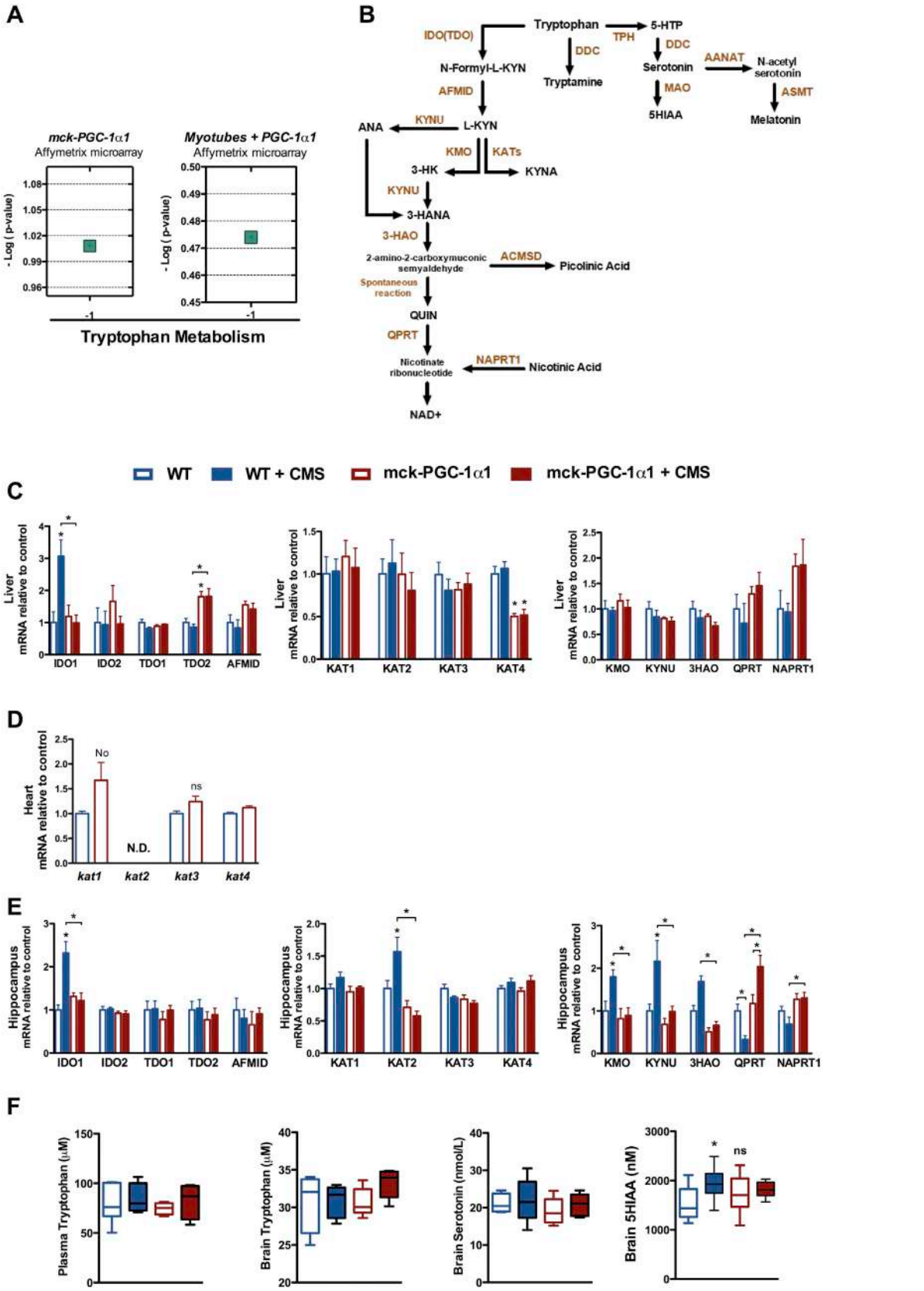

(legend on next page)

Figure S3. PGC-1α1 Regulates Tryptophan Metabolism in Skeletal Muscle, Related to Figure 3

(A) Ingenuity pathway analysis (IPA) of affymetrix-based gene expression arrays where PGC-1α1 was overexpressed in either skeletal muscle (mck-PGC-1α1; in vivo) or in myotubes (+PGC-1α1; in vitro).

(B) Schematic representation of the tryptophan metabolism pathway. Adapted from IPA and Kyoto encyclopedia of genes and genomes (KEGG) pathway database.

(C and D) Analysis of gene expression in liver by qRT-PCR using primers specific to the indicated genes (n = 5-8).

(E) Analysis of gene expression in hippocampus by qRT-PCR using primers specific for the indicated genes (n = 4-6).

(F) Plasma tryptophan levels and brain tryptophan, serotonin, and 5-hydrohyindoleacetic acid (5HIAA) concentrations (n = 4-5). Bars depict mean values and error bars indicate SEM ns nonsignificant, *$p < 0.05$.

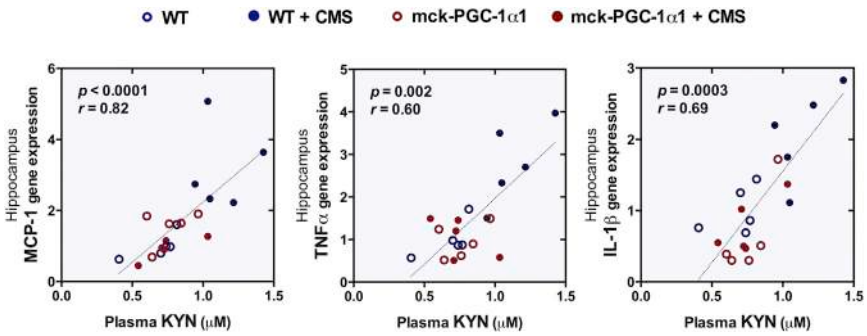

Figure S4. Peripheral Kynurenine Concentrations Correlate with Brain Expression of Proinflammatory Markers, Related to Figure 4

Correlation between plasma KYN levels and hippocampal gene expression proinflammatory markers in animals who underwent chronic mild stress (same animals as in Figures 1, 2, and 3) with each circle representing an individual animal (n = 20-24).

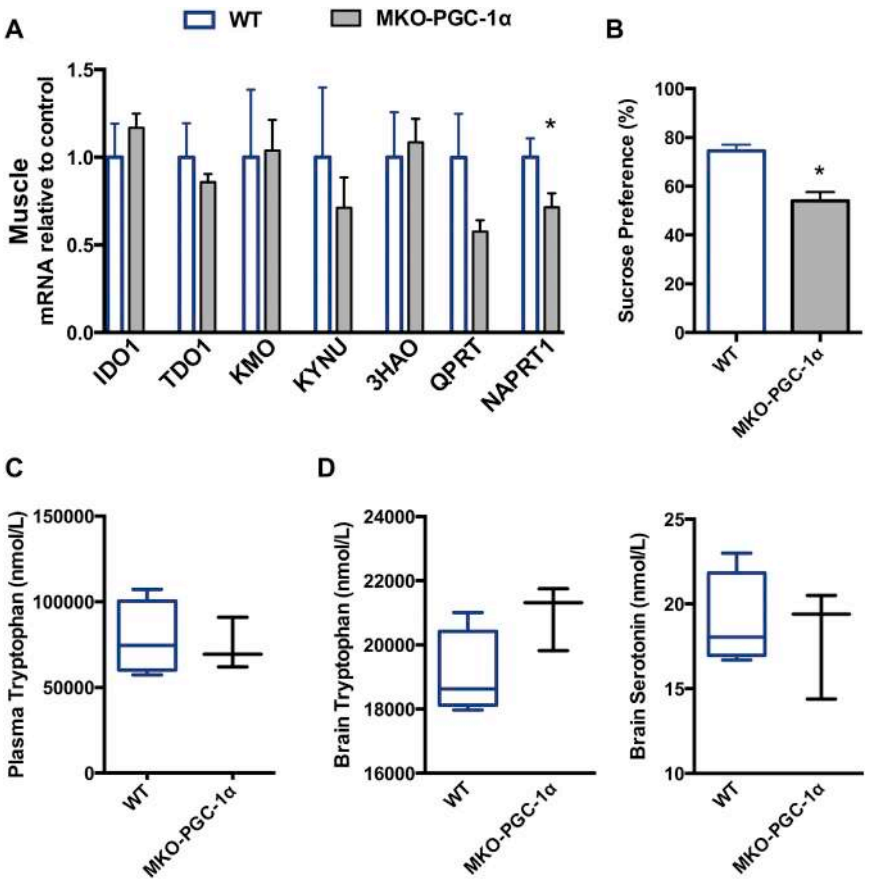

Figure S5. Kynurenine Pathway in Mice with Muscle-Specific PGC-1α Deletion, Related to Figure 5

(A) Analysis of gene expression by qRT-PCR using primers specific to the indicated genes in gastrocnemius muscle from WT and muscle-specific PGC-1α knockout mice (MKO; n = 4-6).

(B) Sucrose preference of the indicated groups (n = 3-5).

(C and D) Plasma tryptophan levels, brain serotonin and brain tryptophan concentration Bars depict mean values and error bars indicate SEM. *$p < 0.05$.

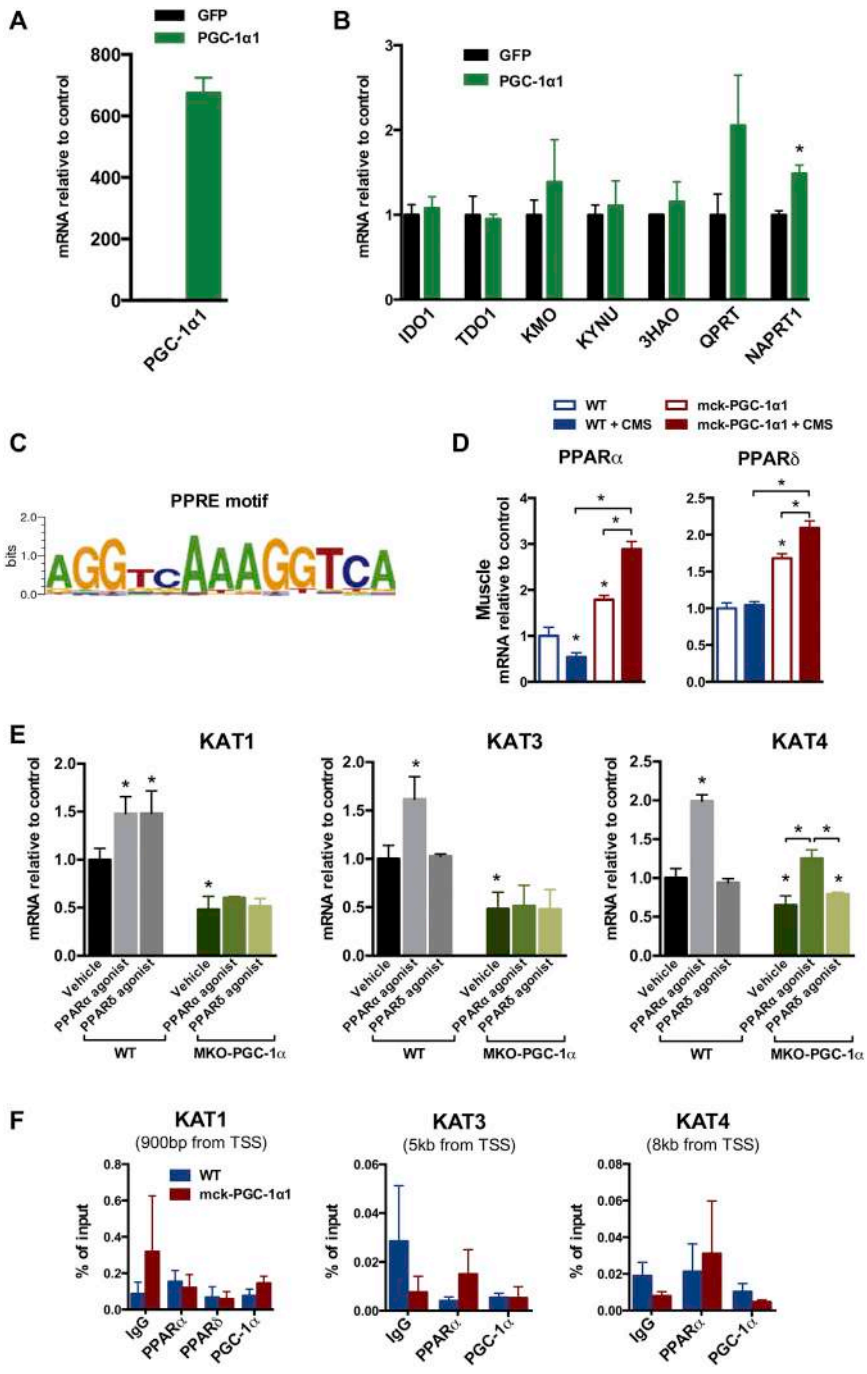

Figure S6. Kynurenine Pathway in Myotubes, Related to Figure 6

(A and B) Gene expression analysis by qRT-PCR using primers specific to the indicated genes. Myotube cultures were transduced with adenoviruses expressing GFP alone or together with PGC-1α1 (n = 3).

(C) Schematic representation of the PPRE consensus sequence.

(D) PPARα and PPARδ mRNA levels in skeletal muscle of WT and PGC-1α1 muscle-specific transgenic mice (mck-PGC-1α1) with or without CMS.

(E) KAT mRNA levels in myotubes derived from WT or MKO-PGC-1α mice treated with vehicle, or selective PPARα or PPARδ agonists (n = 3).

(F) Chromatin immunoprecipitation experiments showing PPARα, PPARδ, and PGC-1α occupancy on KAT gene regulatory regions in skeletal muscle from WT and mck-PGC-1α1 animals (n = 4-6). Bars depict mean values and error bars indicate SD for in vitro and SEM for in vivo experiments. *p < 0.05. Transcription start site (TSS), PPAR-responsive element (PPRE).

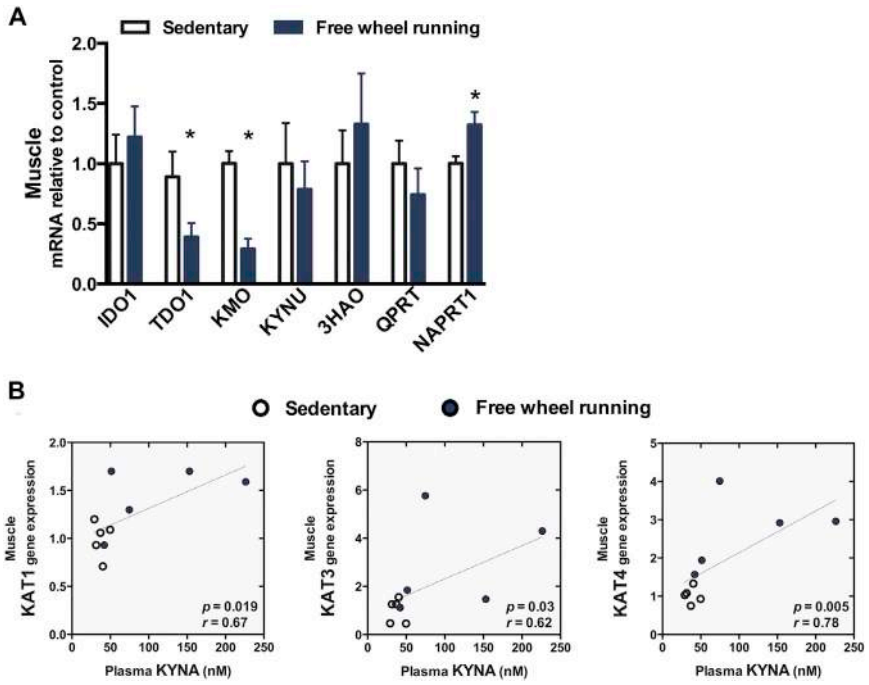

Figure S7. Peripheral Kynurenic Acid Concentrations Correlate with KAT Gene Expression in Skeletal Muscle, Related to Figure 7

(A) Analysis of gene expression by qRT-PCR in gastrocnemius from sedentary and exercise-trained WT mice (n > 5).

(B) Correlation between plasma KYNA levels and gene expression of KAT1, KAT3, and KAT4 in skeletal muscle (n = 10). Bars depict mean values and error bars indicate SEM. *p < 0.05.